

**BONE-DERIVED STEM CELLS REPAIR THE HEART AFTER MYOCARDIAL  
INFARCTION THROUGH TRANSDIFFERENTIATION AND  
PARACRINE SIGNALING MECHANISMS**

---

A Dissertation  
Submitted  
to the Temple University Graduate Board

---

In Partial Fulfillment  
of the Requirements for the Degree of  
Doctor of Philosophy

---

By  
**Jason M. Duran**  
May, 2015

Examining Committee Members:

**Advisor:** Steven R. Houser, PhD; Cardiovascular Research Center  
Michael Autieri, PhD; Cardiovascular Research Center  
Rosario Scalia, MD, PhD; Cardiovascular Research Center  
Emily Tsai, MD; Cardiovascular Research Center  
Marcello Rota, PhD; Brigham and Women's Hospital, Harvard Medical School

UMI Number: 3604669

All rights reserved

INFORMATION TO ALL USERS

The quality of this reproduction is dependent upon the quality of the copy submitted.

In the unlikely event that the author did not send a complete manuscript and there are missing pages, these will be noted. Also, if material had to be removed, a note will indicate the deletion.



UMI 3604669

Published by ProQuest LLC (2013). Copyright in the Dissertation held by the Author.

Microform Edition © ProQuest LLC.

All rights reserved. This work is protected against unauthorized copying under Title 17, United States Code



ProQuest LLC.  
789 East Eisenhower Parkway  
P.O. Box 1346  
Ann Arbor, MI 48106 - 1346

## ABSTRACT

*Rationale:* Autologous bone marrow- or cardiac-derived stem cell therapy for heart disease has demonstrated safety and efficacy in clinical trials but has only offered limited functional improvements. Finding the optimal stem cell type best suited for cardiac regeneration remains a key goal toward improving clinical outcomes.

*Objective:* To determine the mechanism by which novel bone-derived stem cells support the injured heart.

*Methods and Results:* Cortical bone stem cells (CBSCs) and cardiac-derived stem cells (CDCs) were isolated from EGFP+ transgenic mice and were shown to express c-kit and Sca-1 as well as 8 paracrine factors involved in cardioprotection, angiogenesis and stem cell function. Wild-type C57BL/6 mice underwent sham operation (n=21) or myocardial infarction (MI) with injection of CBSCs (n=57), CDCs (n=31) or saline (n=57). Cardiac function was monitored using echocardiography with strain analysis. EGFP+ CBSCs *in vivo* were shown to express only 2/8 factors tested (basic fibroblast growth factor and vascular endothelial growth factor) and this expression was associated with increased neovascularization of the infarct border zone. CBSC and CDC therapy improved survival, cardiac function, attenuated adverse remodeling, and decreased infarct size relative to saline-treated MI controls. CBSC treated animals showed the most pronounced improvements in all parameters. By 6 weeks post-MI, EGFP+ cardiomyocytes, vascular smooth muscle cells and endothelial cells could be

identified on histology in CBSC-treated animals but not in CDC-treated animals. EGFP+ myocytes isolated from CBSC-treated animals were smaller, more frequently mononucleated, and demonstrated fractional shortening and calcium currents indistinguishable from EGFP- myocytes from the same hearts.

Conclusions: CBSCs improve survival, cardiac function, and attenuate remodeling more so than CDCs and this occurs through two mechanisms: 1) secretion of the proangiogenic factors bFGF and VEGF (which stimulates endogenous neovascularization), and 2) differentiation into functional adult myocytes and vascular cells.

## **ACKNOWLEDGEMENTS**

I would like to thank my family and friends for their support during these past few years of research. I want to especially thank my husband Casey for giving me endless support and enduring all of the strains of graduate school first hand. I want to thank my mother Lise for interesting me in science at young age and for sharing all her wisdom about scientific research and the trials of completing a PhD. I also want to thank my father Stan and brother Nate for their continued support.

I could not have completed any of this work without the excellent mentorship of Dr. Steven Houser, the best boss anyone could hope to work for. Dr. Houser and all members of his laboratory were invaluable towards completing this research. My fellow graduate student, Catherine Makarewich, provided friendly support as well as help with molecular biology and myocyte physiology experiments. Dr. Hajime Kubo provided scientific expertise and input across all aspects of this project, and none of this project could have been accomplished without help from him or from our lab manager, Mr. Remus Berretta. Also, I want to give a special thanks to Thomas Sharp for help with stem cell isolation and culture, and to Timothy Starosta, Yumi Chiba, and Sharmeen Husain for all their help with histology.

This project would have been impossible without the help of our invaluable collaborator, Dr. Piero Anversa, a world expert in the field of cardiac repair who shocked the field years ago with his “wild” idea that the heart actually had the

capacity to regenerate. After 15 years, my work and the work of many others has continued to validate what he has been saying all along. Thank you to the members of his team at Brigham and Women's hospital including Dr. Marcello Rota, who taught me all the techniques involved in a mouse model of myocardial infarction and stem cell transplant, Dr. Annarosa Leri for continued assistance with stem cell characterization, Dr. Toru Hosoda for help with stem cell isolation, and Dr. Jan Kajstura (who is, in my opinion, the best histologist in the world).

I would also like to thank my collaborators at Temple, Dr. Madesh Muniswamy and his student Nicholas Hoffman, Dr. Mike Autieri, his student Ross England and his lab manager Sheri Kelemen, and the members of Fox Chase Cancer Center's Biostatistics and Bioinformatics Core; Dr. Eric Ross and Dr. Fang Zhu, who helped me develop statistical models for all of my experiments. I would like to thank Liz Opalka and Lewis Holt-Bright, members of Temple's University Lab Animal Research Facility who helped care for my research animals during the course of my experiments. I also must thank my committee members for their continued help and guidance: Dr. Emily Tsai and Dr. Rosario Scalia in addition to Drs. Rota and Autieri who have already been mentioned. Finally I must thank Dr. Dianne Soprano and Tracey Hinton who run Temple's MD/PhD program. Dr. Soprano gave me an incredible opportunity to join the program here at Temple, and I will be forever thankful to her for allowing me to fulfill my dream of becoming a physician scientist.

## TABLE OF CONTENTS

	<u>Page</u>
<b>ABSTRACT</b>	<b>III</b>
<b>ACKNOWLEDGEMENTS</b>	<b>V</b>
<b>LIST OF TABLES</b>	<b>VIII</b>
<b>LIST OF FIGURES</b>	<b>IX</b>
<b>CHAPTERS:</b>	
<b>1: CLINICAL USES OF STEM CELLS TO TREAT HEART DISEASE</b>	<b>1</b>
<b>2: MECHANISMS OF STEM CELL REPAIR</b>	<b>14</b>
<b>3: MATERIALS AND METHODS</b>	<b>17</b>
<b>4: STEM CELL CHARACTERIZATION <i>IN VITRO</i></b>	<b>29</b>
<b>5: STEM CELLS SUPPORT THE INJURED HEART <i>IN VIVO</i></b>	<b>37</b>
<b>6: EVIDENCE OF PARACRINE FACTOR SECRETION BY STEM CELLS <i>IN VIVO</i></b>	<b>47</b>
<b>7: EVIDENCE OF TRANSDIFFERENTIATION <i>IN VIVO</i></b>	<b>53</b>
<b>8: DISCUSSION</b>	<b>68</b>
<b>9: FUTURE DIRECTIONS FOR CARDIAC CELL THERAPY</b>	<b>76</b>
<b>REFERENCES</b>	<b>72</b>

## LIST OF TABLES

	<u>Page</u>
<i>Table 1: Clinical Trial Design</i>	2
<i>Table 2: Outcome of Clinical Trials</i>	4

## LIST OF FIGURES

	<u>Page</u>
<u>Figure 1: Characterization of stem cells using quantitative real-time PCR</u>	29
<u>Figure 2: Characterization of stem cells by immunostaining</u>	30
<u>Figure 3: Characterization of cortical bone stem cells using flow cytometry</u>	31
<u>Figure 4: In vitro characterization of stem cells</u>	34
<u>Figure 5: Bone-derived stem cells differentiate in vitro</u>	36
<u>Figure 6: 6 week survival</u>	37
<u>Figure 7: Cardiac function measured by echocardiography</u>	39
<u>Figure 8: Infarct size analysis</u>	41
<u>Figure 9: Left ventricular endomyocardial strain</u>	44
<u>Figure 10: Diagram of strain analysis measurements</u>	45
<u>Figure 11: Characterization of paracrine factors secreted by stem cells after 24 hours post-MI in vivo</u>	48
<u>Figure 12: Characterization of paracrine factors secreted by cortical bone stem cells in vivo 2 weeks after MI</u>	49
<u>Figure 13: Stem cell-treated animals have increased von Willebrand Factor+ blood vessels near the infarct border zone by 6 weeks post-MI</u>	50
<u>Figure 14: Expansion of EGFP+ CBSCs as stem cells engraft, align, and elongate over 6 weeks</u>	54
<u>Figure 15: Stem cells grow and differentiate over 6 weeks</u>	55
<u>Figure 16: Individual channel images and staining controls from Figure 15A</u>	56
<u>Figure 17: Low magnification images showin EGFP+ and EGFP- regions of myocardium</u>	57
<u>Figure 18: Low magnification images showing EGFP+ and EGFP- regions around vasculature</u>	58

<u>Figure 19: Individual color channel images and staining controls for Figure 15C</u>	60
<u>Figure 20: Individual channel images and staining controls for Figure 15D</u>	61
<u>Figure 21: Cardiac stem cells grow and expand over 6 weeks but do not adopt a myocyte or vascular phenotype</u>	63
<u>Figure 22: Isolated myocyte size, number of nuclei, and cell physiology were analyzed 6 weeks post-MI</u>	65

## CHAPTER 1: CLINICAL USES OF STEM CELLS TO TREAT HEART DISEASE

Ischemic injury of the heart, including myocardial infarction (MI), is a major health problem that leads to structural and functional remodeling<sup>1</sup> and often culminates in heart failure.<sup>2</sup> Novel therapies to repair or replace damaged cardiac tissue are needed to improve the prognosis of MI patients. Stem cell therapy has the potential to repair hearts after ischemic injury. A variety of adult stem cell types that might repair the injured heart have been tested in animal models with some success, ranging from autologous cardiac<sup>3-6</sup> or bone marrow-derived<sup>7, 8</sup> stem cells, induced pluripotent stem cells,<sup>9-12</sup> and by direct reprogramming of endogenous non-stem cells into cardiogenic phenotypes.<sup>13, 14</sup> Early stage clinical trials have largely focused on autologous stem cells due to their ease of isolation and lack of immunogenicity. In this introduction, 24 clinical trials that are either completed or ongoing will be reviewed.

### Design of clinical trials aimed at cardiac regeneration

In the late 1990s, laboratory science began to challenge the old dogma that the heart was a terminally differentiated organ incapable of repair. As labs around the world began discovering new types of adult stem cells with cardiogenic potential, many clinical trials were initiated. Over the past 15 years, the majority of these trials have focused on adult-derived stem cells, since these avoid the ethical and political controversies of embryonic or fetal-derived stem

**Table 1: Clinical Trial Design**

<b>Study Name</b>	<b>Design</b>	<b>n</b>	<b>Cell Delivery</b>	
Strauer 2002 <sup>15</sup>	NR, C	20 (10/10)	BMC	IC
TOPCARE-AMI, Assmus 2002 <sup>16-18</sup>	R, NC	59 (29/30)	BMC	IC
			PBC	
Stamm 2003 <sup>19</sup>	NR, NC	6	BMC	IM
Perin 2003 <sup>20</sup>	NR, C	21 (14/7)	BMC	TE
Kuethe 2004 <sup>21</sup>	NR, NC	5	BMC	IC
Chen 2004 <sup>22</sup>	RC	69 (34/35)	MSC	IC
BOOST, Wollert 2004 <sup>23,</sup> <sup>24</sup>	RC	60 (30/30)	BMC	IC
Bartunek 2005 <sup>25</sup>	NR, C	35 (19/16)	BMC	IC
IACT, Strauer 2005 <sup>26</sup>	RC	36 (18/18)	BMC	IC
Janssens 2006 <sup>27</sup>	RC	67 (33/34)	BMC	IC
TCT-STAMI, Ge 2006 <sup>28</sup>	RC	20 (10/10)	BMC	IC
ASTAMI, Lunde 2006 <sup>29</sup>	RC	100 (50/50)	BMC	IC
REPAIR-AMI, Schachinger 2006 <sup>30-33</sup>	RC	204 (101/103)	BMC	IC
Meluzin 2006 <sup>34</sup>	RC	66 (22/22/22)	LD BMC	IC
			HD BMC	
Penicka 2007 <sup>35</sup>	RC	27 (17/10)	BMC	IC
TACT-PB-AMI, Tatsumi 2007 <sup>36</sup>	NR, C	54 (18/36)	PBC	IC
Cao 2009 <sup>37</sup>	RC	86 (41/45)	BMC	IC
BALANCE, Yousef 2009 <sup>38</sup>	NR, C	124 (62/62)	BMC	IC
Yao 2009 <sup>39</sup>	RC	39 (12/15/12)	1X BMC	IC
			2X BMC	
TAC-HFT, Williams 2011 <sup>40, 41*</sup>	NR, NC	8 (4/4)	BMC MSC	TE
SCIPIO, Bolli 2011 <sup>42*</sup>	RC	23 (16/7)	CDC	IC
CADUCEUS, Makkar 2012 <sup>43*</sup>	RC	25 (17/8)	CS	IC
FOCUS-CCTRN, Perin 2012 <sup>44</sup>	RC	92 (61/31)	BMC	TE
TIME, Traverse 2012 <sup>45</sup>	RC	67 (43/24) = d3 53 (36/17) = d7	BMC	IC

**Table 1: Clinical trial design.** The basic design of the studies, the total number of patients enrolled, type of cells injected and the mode of delivery used for treatment are shown. Abbreviations: R = Randomized, NR = Non-randomized, C = Controlled, NC = Not Controlled, n = patients per group (treatment/control: for multiple treatments the number per treatment group are listed in order with the number in the control group listed last), d3 = stem cell therapy administered 3 days post-PCI (TIME trial), d7 = stem cell therapy administered 7 days post-PCI (TIME trial), BMC = Bone Marrow-derived mononuclear Stem Cells, PBC = Peripheral Blood-derived mononuclear Stem Cells, CDC = Cardiac-derived Stem Cells, CS = Cardiospheres, LD = Low Dose, HD = High Dose, 1X = Single Dose, 2X = Repeat Dose (at 4 months post-MI), IM = Intramuscular, IC = Intracoronary, TE = transendocardial, yr = years, m = months, wk = weeks

**Table 2: Outcome of Clinical Trials**

Study Name	1° Endpoint	% Change in LVEF		2° Endpoints
		v. Base	v. Ctrl	
Strauer 2002 <sup>15</sup>	3m LVG	+2%	0%	↓ IS
TOPCARE-AMI, Assmus 2002 <sup>16-18</sup>	4m LVG	+8%	NC	↓ IS (MRI 1yr)
		+8%	NC	
Stamm 2003 <sup>19</sup>	2wk Echo	+13%	NC	↓ PD (SPECT)
Perin 2003 <sup>20</sup>	2m Echo	+6%	+4%	↑ WM (EMM)
	4m LVG	+9%	--	
Kuethe 2004 <sup>21</sup>	1yr Echo	-1%	NC	--
Chen 2004 <sup>22</sup>	6m Echo	+18%	+12%	↑ WM (EMM)
BOOST, Wollert 2004 <sup>23, 24</sup>	6m MRI	+7%	+6%	↑ WM
		-3%	-1%	
Bartunek 2005 <sup>25</sup>	4m LVG	+7%	+3%	↑ Glucose uptake, ↓ PD (PET)
IACT, Strauer 2005 <sup>26</sup>	3m LVG	+9%	+8%	↓ IS
Janssens 2006 <sup>27</sup>	4m MRI	+3%	+1%	↓ IS
TCT-STAMI, Ge 2006 <sup>28</sup>	6m Echo	+5%	+7%	↓ PD (SPECT)
ASTAMI, Lunde 2006 <sup>29</sup>	6m	SPECT	+8%	No Difference in EDV, Infarct Size (v. Ctrl)
		Echo	+3%	
		MRI	+1%	
REPAIR-AMI, Schachinger 2006 <sup>30-33</sup>	4m LVG	+6%	+3%	↑ Survival, clinical outcome
	2yr MRI	+5%	+6%	
Meluzin 2006 <sup>34</sup>	3m SPECT	+3%	+1%	↑ Contraction Velocity
		+5%	+2%	
Penicka 2007 <sup>35</sup>	4m Echo	+6%	0%	--
TACT-PB-AMI, Tatsumi 2007 <sup>36</sup>	6m LVG	+13%	+6%	↓ PD (SPECT)
Cao 2009 <sup>37</sup>	4yr Echo	+11.5%	+4%	↓ ESV, ESV
BALANCE, Yousef 2009 <sup>38</sup>	3m LVG	+8%	+7%	↓ IS, ↑ Contraction Velocity
	5yr LVG	+5%	+11%	
Yao 2009 <sup>39</sup>	1yr MRI (1x)	+5%	+3%	↓ IS, ↓ PD (SPECT)
	1yr MRI (2x)	+7%	+5%	

**Table 2: Outcome of Clinical Trials (continued)**

TAC-HFT, Williams 2011 <sup>40,</sup> <sup>41*</sup>	1yr	MRI	0	NC	↓ IS, EDV and ESV
SCIPIO, Bolli 2011 <sup>42*</sup>	4m 1yr	3D Echo 3D Echo	+8% +12%	+8% --	↓ IS
CADUCEUS, Makkar 2012 <sup>43*</sup>	6m	MRI	+1%	0%	↓ IS
FOCUS- CCTRN, Perin 2012 <sup>44#</sup>	6m	Echo	+1%	+3%	No change in ESV or PD (SPECT)
TIME, Traverse 2012 <sup>45</sup>	6m 6m	MRI (d3) MRI (d7)	+4% +3%	-1% +1%	No change in d3 v. d7

**Table 2: Outcome of Clinical Trials.** The primary outcome of each study was determined based on % Change in LVEF versus control groups. The % Change in LVEF over baseline is also shown for comparison in trials that were not properly controlled against a placebo. \*Preliminary results of ongoing clinical trials (TAC-HFT, SCIPIO, CADUCEUS). #FOCUS-CCTRN Primary endpoint was ESV, PD, and myocardial oxygen consumption (not LVEF). Abbreviations: Base = Baseline, Ctrl = Control, LVG = Left Ventriculography, Echo = Echocardiography, MRI = Magnetic Resonance Imaging, SPECT = Single-photon Emission Computed Tomography, PET = positron emission tomography (using FDG-Glucose), IS = Infarct Size, PD = Perfusion Defect, WM = Wall Motion

cells. Additionally, the use of autologous transplants circumvents the risk of immune rejection because the stem cells being transplanted are derived from one's own body.

In Table 1 and 2, some of the most important clinical trials using autologous stem cell transplants are described. Table 1 gives an overview of the trial designs, listing whether the trials were appropriately controlled against a placebo treatment (C = controlled, NC = not controlled) and whether patients were appropriately randomized into treatment or control groups (R = Randomized, NR = not randomized, RC = randomized and controlled). Although some earlier trials were not properly placebo controlled, they were important in proving that stem cells are safe for use in human studies to treat heart disease. TOPCARE-AMI 2002<sup>16</sup>, although not controlled, demonstrated positive improvements in LVEF over baseline measurements and showed that bone marrow-derived mononuclear stem cells (BMCs) or peripheral blood-derived mononuclear stem cells (PBCs) could be safely delivered by intracoronary infusion without inducing arrhythmias or any adverse inflammatory response. Another trial that was not placebo controlled, Kuethe 2004<sup>21</sup>, failed to demonstrate positive functional improvements over baseline measurements after intracoronary BMC therapy, but importantly the trial reported no adverse effects of cell therapy.

### Stem Cell Delivery

These trials have utilized several different strategies for delivering stem cells to the heart to help repair cardiac tissue injury. Older trials<sup>19</sup> relied on direct intramuscular injection of cells into the heart after thoracotomy or sternotomy, but this is a highly invasive strategy that is no longer necessary with recent improvements in interventional technology. Most studies since have relied on two different interventional delivery mechanisms: intracoronary (IC) infusion of stem cells through an over-the-wire balloon catheter, or transendocardial (TE) injection of stem cells directly into the ischemic myocardium from inside the left ventricular chamber. Animal studies have suggested that intramuscular injection may offer greater retention of stem cells than intracoronary infusion<sup>46-48</sup>, but both delivery methods have shown promising results in clinical trials. Perin 2003<sup>20</sup> reported positive recovery in left ventricular ejection fraction (LVEF) and wall motion velocity 2-4 months after TE injection of BMCs, while the TCT-STAMI Trial 2006<sup>28</sup> reported positive recovery of LVEF and decreased perfusion defect 6 months after IC infusion of BMCs. However, IC infusion has been much more widely tested than TE injection, and it has proven safe for use in 18/22 of the clinical trials listed in Table 1.

Within several trials, specific aspects of stem cell delivery have been tested, such as the number of cells delivered, number of doses to be delivered, and timing of stem cell delivery. One trial (Meluzin 2006<sup>34</sup>) directly compared a low-dose ( $1 \times 10^7$  cells/patient) and a high dose ( $10 \times 10^7$  cells/patient) of BMCs within a single trial. Although the high dose of stem cells did show a slightly

greater improvement in LVEF (+2% vs. placebo), this improvement was only modestly higher than the low dose (+1% vs. placebo). Additionally, a meta-analyses of all 24 trials listed in Table 1 and 2, which range in cell dose from as few as  $1 \times 10^6$  (SCIPIO 2011<sup>42</sup>) to as high as  $9 \times 10^9$  (Chen 2004<sup>22</sup>), failed to establish any dose response relationship between the number of cells delivered and the primary clinical outcome (positive changes in LVEF over the placebo group was used as the primary endpoint in most of the trials listed in Table 2). Another trial examined the effect of a single versus repeated doses of stem cells (Yao 2009<sup>39</sup>), and found that patients receiving a second dose of cells had greater improvements in LVEF over placebo (+5%) compared to the single dose group (+3%) measured by MRI 1 year after intervention.

Timing of stem cell delivery after injury may also be crucial. Most of these trials have focused on administration of stem cells within the first week after percutaneous coronary intervention (PCI) was performed to reperfuse an acute MI, and one trial was designed to find the optimal time for administration of stem cells to treat acute MI within the first week after injury (TIME 2012<sup>45</sup>). This trial directly compared stem cell infusion at 3 days post-PCI to 7 days post-PCI and was unable to demonstrate any significant improvement in LVEF in either group measured by MRI 6 months after intervention. However, other trials administering cells near 3 days post-PCI (TACT-PB-AMI 2007<sup>36</sup>, 2.5 days post-PCI, +6% LVEF; REPAIR-AMI<sup>30, 31</sup> 2006, 4.5 days post-PCI, +3% LVEF) and near 7 days post-PCI (Cao 2009<sup>37</sup>, 7 days post-PCI, +4% LVEF; BALANCE<sup>38</sup>, 7 days post-PCI, +11% LVEF) all demonstrated positive changes in primary

outcomes regardless of the timing of cell therapy, conflicting with the results of the TIME trial. Additionally, several trials have administered cells to patients suffering from chronic ischemic heart disease for several years. The IACT 2005<sup>26</sup> trial demonstrated +8% improvement in LVEF over placebo, while the ongoing SCIPION 2011<sup>42</sup> trial, on which preliminary results of the first 16 controlled patients were recently published, also showed a +8% improvement in LVEF. Thus, these two trials show that stem cells offer functional benefit even when delivered into chronically scarred and ischemic myocardium.

#### *Interpreting Clinical Trial Outcomes*

The clinical outcomes presented in Table 2 show that, while safety and efficacy are not a major concern with IC or TE-delivered cell therapies, results have been mixed and are difficult to interpret. Most trials listed in Table 2 used LVEF as the primary outcome (with the exception of FOCUS-CCTR 2012,<sup>44</sup> which used LV end-systolic volume), and secondary outcomes included infarct size, ventricular dimensions, myocardial perfusion scores or wall motion measurements. While a few trials reported that stem cell therapy imparted no functional benefit or improvement in any secondary endpoints (ASTAMI 2006<sup>29</sup>, Penicka 2007<sup>35</sup>, TIME 2012<sup>49</sup>), other trials that reported no functional benefit did show some improvements in secondary endpoint parameters. Strauer 2002<sup>15</sup> and Janssens 2006<sup>27</sup> reported no functional improvement in LVEF of BMC-treated patients over placebo-treated patients, but both trials showed decreased infarct size in the BMC group (measured by left ventriculography 3 months after

cell therapy in Strauer 2002, or measured by MRI 4 months after cell therapy in Janssens 2006). The TAC-HFT 2011<sup>40</sup> trial was a preliminary phase I trial designed to compare BMCs directly to mesenchymal stem cells (MSCs), which are the adherent stem cells that grow out of bone marrow mononuclear cell cultures. Although small and not properly controlled, this trial showed no functional improvements over baseline but did demonstrate decreased infarct size and reverse remodeling on MRI 1 year after therapy with either cell type (the trial was not adequately powered to detect significant differences between BMC- and MSC-treated patients). Likewise, the ongoing CADUCEUS 2012<sup>43</sup> trial showed that, by 1 year after cardiosphere therapy, LVEF was not significantly better in the treatment group than in placebo controls, but infarct size was significantly decreased as measured by 3D echocardiography.

There is additional controversy as to whether these functional changes can be sustained over time. Three of the largest trials that were properly randomized and controlled are now completed and have several years of follow-up data to compare. The BOOST 2004<sup>23, 24</sup> trial was completed with 30 patients receiving BMC therapy and 30 receiving placebo. At 6 months after therapy, patients in the treatment arm demonstrated 6% improvement in LVEF over placebo measured by MRI and increased wall motion at the infarct border zone measured by electromechanical mapping. However, serial MRI measurements demonstrated a progressive decrease in LVEF in the treatment arm so that by 5 years after therapy there was no longer any significant difference between the

treatment and placebo groups. Additionally BMC-treated patients experienced adverse cardiac events at a similar frequency to those in the placebo group.

Two of the other largest studies, in contrast to the BOOST trial, have demonstrated functional improvements that were sustained long-term. REPAIR-AMI 2006<sup>30, 31</sup>, the largest clinical trial completed to date with 101 patients receiving intracoronary BMCs and 103 receiving placebo, demonstrated initial +3% improvements in LVEF measured 4 months after cell therapy by left ventriculography. The more recently published 1 year<sup>33</sup> and 2 year<sup>32</sup> follow-ups have demonstrated that these functional improvements were sustained, and that there was improved survival (only 3/100 deaths in the BMC treatment group compared to 8/101 in the placebo group) and decreased rates of adverse cardiac events following BMC therapy. The BALANCE 2009 trial, in which 62 patients received intracoronary BMCs and 62 received placebo, also demonstrated early improvements in LVEF (+7% versus placebo after 3 months) that sustained over time (+10% versus placebo after 5 years). Additionally infarct sizes were smaller and systolic contraction velocities were improved in the BMC treatment group relative to placebo controls.

#### Finding the right stem cell for cardiac regeneration

A critical aspect to developing more successful regenerative strategies in future trials will be determining the optimum cell type to induce repair. Five types of autologous stem cells have been tested thus far in the clinical setting: bone marrow-derived mononuclear cells (BMC), peripheral blood-derived mononuclear

cells (PBC), bone-marrow derived mesenchymal stem cells (MSCs), cardiac-derived stem cells sorted for c-kit+ (CDCs), or cardiospheres (CSs), a mixture of unsorted cells that grow into spheres *in vitro* out of cardiac biopsies. Of the five types, bone marrow mononuclear cells have been most widely tested. In the 19 trials listed in Tables 1 and 2, these cells have been safely used in over 650 patients. However, the mixed results from these 19 trials may be due to the heterogeneity of the cells in a bone marrow mononuclear cell preparation, which are isolated by simple density gradient centrifugation of bone marrow aspirate to separate the mononuclear cell fraction. Animal studies have demonstrated that the cardiogenic or vasculogenic pool of stem cells in this BMC population is relatively low. CD34+ hematopoietic stem cells with vasculogenic potential may represent less than 2% of all mononuclear cells in the bone marrow and less than 0.1% of cells circulating in peripheral blood,<sup>50</sup> while c-kit+ stem cells with cardiogenic potential may represent less than 5% of all cells in the bone marrow<sup>51</sup> and are even less abundant in the heart. One group counted only 1 c-kit+/lineage- cell for every  $1 \times 10^4$  myocytes in the ventricles,<sup>3</sup> while another group estimated that c-kit+/lineage- cells represent less than 0.04% of cells in the atria.<sup>52</sup>

The only clinical trial that has specifically sorted and expanded stem cells that have been proven through preclinical studies to directly mediate cardiomyogenesis has been the SCiPIO 2011<sup>42</sup> trial, which is currently ongoing. In this trial, c-kit+ cardiac stem cells are isolated from an atrial biopsy and expanded prior to administration to the patient. Although only early results have

been published, this trial has produced a greater improvement in cardiac function than most other trials, demonstrating over +8% improvement in LVEF versus placebo. Other earlier trials have attempted to quantify the number of specific cardiogenic or vasculogenic stem cells in their heterogenous populations of BMCs or PBCs (for example, Bartunek 2005<sup>25</sup> determined their cell populations to be 70% CD133+, a marker of a sub-population of CD34+ hematopoietic stem cells), but they did not actually sort for or purify these cells.

Thus, while the outcomes of these trials continue to improve, the overall beneficial effects of autologous stem cell therapies are still relatively modest and the fundamental mechanisms of stem cell mediated repair are largely unknown and controversial. Our current study seeks to address the major mechanisms of stem cell-mediated repair of the heart in a novel population of cortical-bone derived c-kit+/Sca-1+ stem cells.

## CHAPTER 2: MECHANISMS OF STEM CELL REPAIR

The mechanisms of stem cell-mediated cardiac repair are critical unanswered questions in the field. Many preclinical studies in animal models have shown that differentiation<sup>6-8</sup> of injected cells into new cardiac myocytes is one potential mechanism of this repair. Secretion of paracrine factors that enhance cardioprotection of the endogenous myocardium, neovascularization, and recruitment of endogenous stem cells that promote repair are other major mechanisms.<sup>4, 5, 53, 54</sup> The goal of the present study was to define the contributions of differentiation of transplanted bone-derived stem cells into new cardiac tissue (cardiac myocytes and blood vessels) versus stem cell-mediated induction of endogenous cardiac repair via secretion of paracrine factors.

Finding well-characterized sources of stem cells for cardiac regeneration is key to enhance new clinical studies. Certain stem cell types may have a greater capacity to transdifferentiate, while others may produce more paracrine factors and have a greater potential to stimulate neovascularization and other endogenous repair mechanisms. Although a solid consensus is lacking, most cardiac stem cell researchers currently believe that BMCs act primarily through paracrine stimulation of new blood vessel formation or through differentiation into vascular cells rather than transforming to myocytes, while CDCs may differentiate into adult myocytes.<sup>55</sup> Although some studies have demonstrated that BMCs can regenerate adult myocytes<sup>7, 8</sup>, others have suggested that these

new myocytes are mostly formed through stimulation of endogenous cardiac stem cells rather than through direct differentiation of the transplanted cells.<sup>48, 56</sup>

Our goal was to define if and by what mechanisms, bone-derived stem cells induce repair of the injured heart.

It has long been hypothesized that both the heart and bone marrow contain stem cell niches where cells with the capability to differentiate down the cardiac or mesenchymal lineage exist in a dedifferentiated state.<sup>7, 57-59</sup> In these environments, the stem cell's pluripotent state is thought to be supported by complex signaling interactions with surrounding cells, such as those found in the stromal lining of the bone marrow cavity. Investigators looking for a source of multipotent stem cells developed a new isolation technique using bone tissue itself rather than the bone marrow, to isolate cells that might be in a more primitive state.<sup>60</sup> These cells, which can be easily obtained through routine bone biopsy procedures, were negative for most markers of the hematopoietic lineage and expressed the pluripotency marker Sca-1. Under specific culture conditions these cells differentiate *in vitro* into osteoblasts, chondrocytes, and adipocytes<sup>60</sup> but no one has yet tested their cardiogenic potential in the injured heart. In this study, we report for the first time that injection of cortical bone-derived stem cells (CBSCs) into the heart after MI improved survival and cardiac function, and CBSCs demonstrated greater improvements across all parameters compared to the more widely studied CDCs. CBSCs differentiated into new cardiac tissue, while CDCs did not, and CBSCs demonstrated a greater capacity for paracrine-mediated endogenous repair to produce these effects. Our study suggests that

CBSCs are a source of stem cells that are more abundant and more easily isolated than CDCs, and that CBSCs have a greater capacity to repair hearts damaged by ischemic injury.

## CHAPTER 3: MATERIALS AND METHODS

### Animals and Anesthesia

All animal procedures were approved by the Temple University School of Medicine Institutional Animal Care and Use Committee. For all procedures (bone isolation, myocardial infarction, echocardiography, invasive hemodynamics, and cardiectomy) anesthesia was induced using 3% isoflurane and maintained using 1% isoflurane (Butler Shein Animal Health; Dublin, Ohio). Adequate induction of anesthesia was confirmed prior to any intervention by observation of a negative paw- or tail-pinch reflex. For procedures involving a thoracotomy (i.e. myocardial infarction surgeries) animals were intubated after induction of anesthesia and ventilated at a rate of 180-190 breaths per minute and a tidal volume of 250-300 µL (ventilation parameters were adjusted accordingly depending on the size of each animal). For all other procedures, maintenance anesthesia was delivered via nose cone. All animals used for *in vivo* studies were 12-week-old male C57BL/6 mice (The Jackson Laboratory; Bar Harbor, ME).

### Isolation and culture of cortical bone-derived stem cells

Cortical bone stem cells (CBSCs) were isolated using previously published techniques.<sup>60</sup> Femurs and tibias were isolated from transgenic 12-week-old male C57BL/6-Tg(CAG-EGFP)1Osb/J mice (The Jackson Laboratory; Bar Harbor, ME), which constitutively express enhanced green fluorescent protein (EGFP) off of the β-actin promoter in most cells of the body. The

epiphyses of the bones were removed, and the marrow cavity was flushed three times with phosphate-buffered saline (PBS) and the marrow was discarded. The remaining cortical bone was crushed using a sterilized mortar and pestle, and bone fragments were further digested using collagenase II. Bone chunks were then plated in CBSC culture media: DMEM/F12 Media (Lonza/BioWhittaker; Basel, Switzerland) + 10% fetal bovine serum (Gibco Life Technologies; Grand Island, NY), 1% Penicillin/Streptomycin/L-glutamine (Gibco Life Technologies; Grand Island, NY), 0.2% insulin-transferrin-selenium (Lonza; Basel, Switzerland), 0.02% basic-fibroblast growth factor (Peprotech; Rock Hill, NJ), 0.02% epidermal growth factor (Sigma; St. Louis, MO), and 0.01% leukemia inhibitory factor (Millipore; Billerica, MA). Over the first week in culture, fibroblast-like stem cells began to grow out from the bone chunks, and after 1 week in culture, the remaining chunks of bone were washed away and the adherent population of CBSCs could be passaged for expansion. Expanded cells could be resuspended in CBSC culture media + 10% DMSO to be frozen and stored long-term in liquid nitrogen.

#### *Isolation of cardiac-derived stem cells*

Cardiectomy was performed on transgenic 12 week-old male C57BL/6-Tg(CAG-EGFP)1Osb/J mice (The Jackson Laboratory; Bar Harbor, ME) under general anesthesia. Hearts were cannulated and perfusion digested to dissociate stem cells from the left ventricle, and cardiac-derived stem cells (CDCs) underwent sorting for c-kit using magnetic beads (Miltenyi Biotec;

Cologne, Germany) following a previously described protocol.<sup>3, 61</sup> Cells were cultured and stored long term under identical conditions to CBSCs as previously described.

#### *Isolation and Culture of Mouse Left Ventricular Myocytes*

Left ventricular myocytes were isolated from mice receiving MI and CBSC therapy 6 weeks after injection for myocyte staining and cell physiology experiments. Cardiectomy was performed under general anesthesia then hearts were cannulated and perfusion digested with collagenase-containing Tyrodes solution on a constant-flow Langendorff apparatus, and left ventricular myocytes were isolated and cultured as previously described.<sup>62, 63</sup> All myocytes isolated from the left ventricle of each MI+CBSC mouse were plated on laminin-coated 18mm round glass coverslips. Some coverslips were used to measure fractional shortening and calcium transients, others were fixed and immunostained for cell counts, surface area analysis, and nuclei counts.

To estimate the percentage of all LV myocytes that were EGFP+ (and thus derived from injected CBSCs), an average number of  $15.67 \pm 3.67$  EGFP+ myocytes were counted on each coverslip. The total number of myocytes on each coverslip was estimated by counting the myocytes in ten random 10X visual fields, and an average of  $12.4 \pm 1.51$  total myocytes/field were counted. A 10X visual field has a surface area of  $1.30 \text{ mm}^2$ , and an 18mm coverslip has a surface area of  $81\pi \text{ mm}^2$ , so there are  $81\pi/1.30 = 150.18$  10X visual fields/coverslip. Thus there were an average of  $12.4 * 150.18 = 1862.26$  total

myocytes/coverslip. So by 6 weeks post-MI, an estimated  $15.67/1862.26 = 0.84\%$  of myocytes isolated from CBSC-injected animals were EGFP+.

#### Fractional Shortening and Calcium Transients

Mouse left ventricular myocytes isolated from CBSC-injected animals 6 weeks post-MI were simultaneously measured for fractional shortening and calcium transients as has been previously described.<sup>62, 63</sup>

#### Flow Cytometry

For flow cytometry,  $5 \times 10^6$  CBSCs were incubated for 15 minutes at 4°C in under gentle agitation in the appropriate antibody diluted 1:11 in wash buffer (PBS+ 0.5% bovine serum albumin + 2 mM EDTA, pH = 7.3). After incubation, cells were washed with 2 mL wash buffer, centrifuged at 300 Xg for 5 min, and supernatants were aspirated and discarded. Stained cells were resuspended in PBS for flow cytometry. The following conjugated antibodies were used: anti-c-kit-APC, anti-Sca-1-APC and Lineage Cocktail-APC (Miltenyi Biotec; Cologne, Germany), anti-CD29-APC (eBiosciences; San Diego, CA), and CD34-Alexa Fluor 647 and anti-CD45-Alexa Fluor 647 (AbD Serotec; Kidlington, UK). A second sample of CBSCs was stained in each condition with APC-conjugated Rat IgG2b, which was used as a negative isotype control.

### RNA Isolation and PCR Analysis

CDCs or CBSCs were resuspended in QIAzol Lysis Reagent, and mRNA was isolated using an RNeasy Mini Kit. DNA was eliminated from the samples using RNase-free DNase I, and then cDNA was generated using RT<sup>2</sup> First Strand Kit. RT<sup>2</sup> qPCR Primer Assays for mouse Kit (c-kit), mouse Ly-6A (Sca-1), and mouse glyceraldehyde 3-phosphate dehydrogenase (GAPDH) were used with RT<sup>2</sup> SYBR Green qPCR mastermix to detect c-kit, Sca-1, or GAPDH mRNA expression, respectively. The amount of GAPDH mRNA in each cell type was determined using a 6-point standard curve with a 1:10 serial dilution of each transcript run on each primer set. The amount of transcript detected for c-kit or Sca-1 was normalized to detected levels of GAPDH and these data are presented as normalized arbitrary units (NAUs). All qPCR reagents were purchased from Qiagen (Valencia, CA).

### Protein Isolation and Western Analysis

CBSC or CDC lysates were prepared and analyzed using Western analysis as previously described.<sup>63, 64</sup> The following primary antibodies purchased from Abcam (Cambridge, MA), Cell Signaling (Danvers, MA) or AbD Serotec (Kidlington, UK) were used to detect target antigens: insulin-like growth factor-1 (Abcam ab106836), angiopoietin-1 (Abcam ab95230), basic-fibroblast growth factor (Abcam, ab8880), hepatocyte growth factor (Abcam ab83760), platelet-derived growth factor (Abcam ab125268), stem cell factor (Abcam ab9753), stromal-derived factor-1 (Cell Signaling #3740S), vascular endothelial

growth factor (Abcam ab46154) and Glyceraldehyde 3-phosphate dehydrogenase (AbD Serotec) . The following secondary antibodies were used: rabbit-HRP (GE#NA934V) and mouse-HRP (GE#NA931V) purchased from GE Healthcare (Little Chalfont, UK) and goat-HRP (sc-2020) purchased from Santa Cruz Biotechnology (Dallas, TX).

Enzyme-Linked Immunosorbent Assays

CBSCs or CDCs were plated at a low density of 25,000 cells/well in complete CBSC media or serum free media in a 6 well plate and allowed to proliferate to 90% confluence over 72 hours. Serum samples were collected every 24 hours and frozen at -20°C. Samples were analyzed using mouse DuoSet ELISA Kits for hepatocyte growth factor, insulin-like growth factor, stem cell factor, stromal-derived factor-1 and vascular endothelial growth factor. The presence of serum in the cell cultures did not affect cytokine production. All ELISA kits were purchased from R&D Systems (Minneapolis, MN). The data in each case is presented as a mean of 3 samples, and for each ELISA, background signal was subtracted using the mean of 3 samples containing unconditioned media only. A student's T test was used to detect any significant difference in production of each paracrine factor between CBSCs and CDCs.

### In vitro Differentiation Co-cultures

Neonatal rat ventricular myocytes were isolated following the Simpson and Savion protocol<sup>65</sup> with minor modifications that we have previously described.<sup>66</sup>,<sup>67</sup> Cells were plated overnight on gelatin-coated 18mm glass coverslips in a 12-well dish. Stem cells were added the following day at low densities (1000-5000 cells/well) on top of the neonatal rat myocytes. Cells were allowed to differentiate in co-culture for 72 hours. During this time some EGFP+ cells were observed to beat. After 72 hours, coverslips were fixed and stained for α-sarcomeric actin or connexin43.

### Mouse Myocardial Infarction and Intramyocardial Stem Cell Transplantation

Permanent occlusion myocardial infarction (MI) surgery was performed by ligating the left anterior descending coronary artery following a widely cited protocol.<sup>68</sup> Immediately after MI, 40,000 CBSCs (n=57) or CDCs (n=31) suspended in normal saline were injected intramyocardially into the infarct border zone in four x 5 uL injections. MI control animals (n=59) received saline injection only, and sham control animals (n=21) received all surgical procedures except for ligation of the coronary artery and intramyocardial injection.

Of the 57 animals that received MI+CBSC injection, 13 were lost to follow-up during the 6-week course of study. Ten animals were sacrificed at 24 hours post-MI (5 were used for acute infarct size analysis and 5 were perfusion fixed for immunohistochemistry and analysis of *in vivo* paracrine factor expression). The

remaining 21 animals underwent serial echocardiography. Of these animals, 5 were sacrificed 1 week post-MI, 5 animals at 2 weeks post-MI, and 6 animals at 6 weeks post-MI and their hearts were perfusion fixed for immunohistochemistry. Myocytes were isolated from 8 animals at 6 weeks post-MI for immunocytochemistry and electrophysiology. The remaining 5 hearts from MI+CBSC animals were either damaged during cardieotomy or were not properly arrested and fixed and thus could not be used for histological analysis.

Of the 31 animals that received MI+CDC injection, 8 were lost to follow-up during the 6-week course of study. Ten animals were sacrificed at 24 hours post-MI (5 were used for acute infarct size analysis and 5 were perfusion fixed for immunohistochemistry and analysis of *in vivo* paracrine factor expression). The remaining 13 animals underwent serial echocardiography. Of these animals, 6 were sacrificed 1 week post-MI, 3 animals at 2 weeks post-MI, and 4 animals at 6 weeks post-MI and their hearts were perfusion fixed for immunohistochemistry.

Of the 57 animals that received MI+Saline injection, 27 were lost to follow-up. Five animals were sacrificed at 24 hours post-MI for acute infarct size analysis. Of the 23 remaining animals, 6 were sacrificed at 1-week post-MI, 5 were sacrificed at 2 weeks post-MI, 6 were sacrificed at 6 weeks post-MI, and their hearts were perfusion-fixed for immunohistochemistry. The remaining 3 hearts from 6 weeks post-MI+Saline animals were either damaged during cardieotomy or were not properly arrested and fixed and thus could not be used for histological analysis. Of the 21 animals in the sham-operated group, 5 were sacrificed at 1-week post-MI, 5 were sacrificed at 2 weeks post-MI, 5 were

sacrificed at 6 weeks post-MI and all hearts were perfusion-fixed for immunohistochemistry.

#### *Infarct Size Analysis*

After 24 hours post-MI, five animals from each study group (MI+CBSC, MI+CDC, or MI+Saline) were randomly selected to undergo acute infarct size analysis. Cardiectomy was performed under general anesthesia, and the hearts were perfused with 2% Evan's Blue dye in PBS to stain the area at risk (AAR), which accounts for all areas of the myocardium except for those perfused by the ligated coronary artery. The heart was then flash-frozen in liquid nitrogen so it could be cut into 6-8 short-axis cross sections. The sections were washed in PBS to remove excess Evan's Blue dye then incubated in 2% triphenyltetrazolium chloride in PBS for 10 minutes at 37°C to stain ischemic tissues white (ischemic area, IA) and viable tissues red. Samples were washed again in PBS then photographed under a top-lit dissecting scope. AAR and IA were measured on each photograph using NIH image J software, and a mean AAR and IA for each heart was calculated as a percentage of total ventricular area.

For chronic infarct size analysis, paraffin-embedded short-axis heart sections from MI+CBSC, MI+CDC, or MI+Saline sacrificed 6 weeks post-MI were stained with hematoxylin and eosin (H&E). Brightfield photographs were acquired on a dissecting microscope using a DS-Fi1 color camera and NIS Elements software (all from Nikon Inc.; Melville, NY). Pathologically fibrotic and

infarcted regions of the myocardium were identified and their surface area was quantified using NIH Image J software. Infarct area was calculated as a percentage of total ventricular surface area for 3-4 cross-sections

#### *Two-Dimensional Echocardiography and Strain Analysis*

Anesthetized mice underwent transthoracic echocardiography using a Vevo2100 ultrasound system (VisualSonics; Toronto, Canada). Repeated measurements were performed as previously described<sup>62, 69, 70</sup> at baseline and at 1, 2, 4, and 6 weeks post-MI. Images were acquired by JMD in the short-axis B-mode and M-mode for analysis of cardiac function and dimensions. Long-axis B-mode images were recorded for longitudinal and radial strain analysis using the VevoStrain software following a recently published protocol.<sup>71</sup> After echocardiograms were recorded, image series were randomly ordered and renumbered by CAM. All images were analyzed under their coded numbers in a blinded fashion by JMD, then the code was broken by CAM and animal data was analyzed.

#### *Perfusion Fixation*

Cardiectomy was performed under general anesthesia and the heart was rinsed and weighed. The aorta was then cannulated and the coronary arteries were cleared by perfusion with 1 mL cold Krebs-Henseleit Buffer. The heart was then arrested in diastole by perfusion with 1 mL of 100 mM cadmium chloride/1 M potassium chloride solution. The hearts were then gravity perfused with 30 mL

10% formalin at mean arterial pressure (100 mmHg). Fixed hearts were immersed overnight in 10% formalin and then stored in 70% ethanol for up to 1 week before being processed and embedded in paraffin wax blocks.

### Immunohistochemistry

For *in vitro* staining, cells were plated on gelatin-coated coverslips overnight and then fixed with 4% paraformaldehyde. Cells were permeabilized with 0.1% Triton X-100 in PBS (Fluka/Sigma-Aldrich; St. Louis, MO) and stained for the following proteins: c-kit (R&D Systems; Minneapolis, MN), Sca-1 (Miltenyi Biotec; Auburn, CA), insulin-like growth factor-1 (Santa Cruz Biotechnology; Dallas, TX), angiopoietin-1, basic-fibroblast growth factor, hepatocyte growth factor, platelet-derived growth factor, stem cell factor, stromal-derived factor-1, and vascular endothelial growth factor (all purchased from Abcam; Cambridge, MA). For neonatal rat ventricular myocyte co-cultures, cells were stained for α-sarcomeric actin (Sigma; St. Louis, MO) or connexin43 (Millipore; Billerica, MA).

For fixed tissues, wax blocks were cut into 5 µm thick sections that were mounted on glass slides for staining. Slides were deparaffinized and underwent antigen retrieval in hot citric acid buffer. Stains were conducted against the following proteins: α-sarcomeric actin and α-smooth muscle actin (Sigma; St. Louis, MO), EGFP and von Willebrand factor (Abcam; Cambridge, MA), and connexin43 (Millipore; Billerica, MA). Nuclei in both cells and embedded tissues were stained with 4',6-diamidino-2-phenylindole (DAPI, Millipore; Billerica, MA).

### Statistical Analysis

All statistical analyses were overseen by the Fox Chase Cancer Center Biostatistics and Bioinformatics Facility. Survival analysis is presented using a Kaplan-Meier regression and statistical significance was determined using the log-rank test. For infarct size analysis, blood vessel counts and isolated myocyte measurements (where discrete measurements were compared at a single time point), a two-way T test was used. For follow-up parameters with repeated measures (echocardiography and strain analysis), growth curve models with cubic splines were used. All growth curve coefficients were fitted as random effects to allow deviation of individual growth from the mean of the treatment group. Interaction term with the treatment was also included to compare the mean growth rates by treatment. For all statistical tests, a p-value < 0.05 was considered statistically significant.

## CHAPTER 4: STEM CELL CHARACTERIZATION *IN VITRO*

### *Expression of Pluripotency Markers*

Cortical bone stem cells (CBSCs) or cardiac-derived stem cells (CDCs) were analyzed for expression of c-kit and Sca-1 mRNA abundance using quantitative real-time PCR (qPCR), and c-kit and Sca-1 protein levels were detected using both immunostaining and flow cytometry. Levels of c-kit or Sca-1

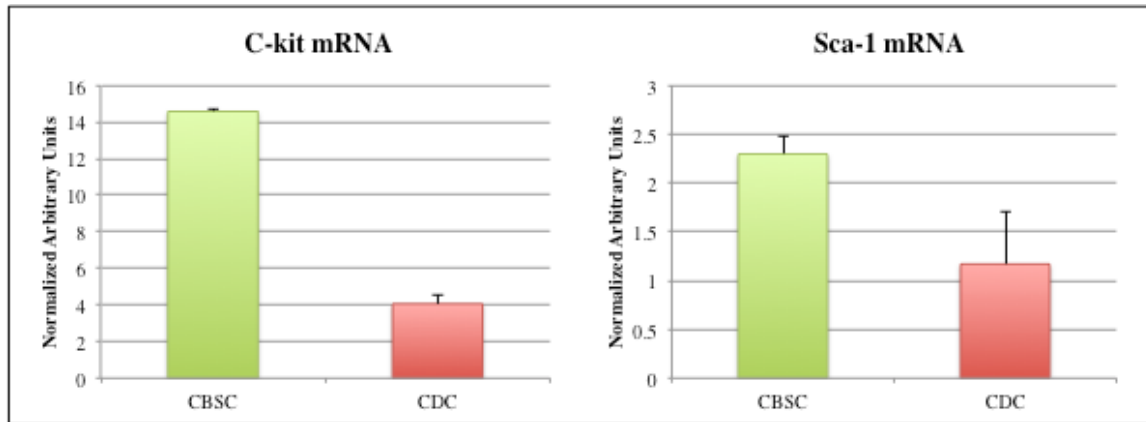


*Figure 1: Characterization of stem cells using quantitative real-time PCR (qPCR).*

qPCR of c-kit and Sca-1 mRNA from cortical bone stem cells (CBSCs) or cardiac-derived stem cells (CDCs) was normalized to levels of GAPDH transcript expressed by each cell type. Results are presented as normalized arbitrary units (NAUs).

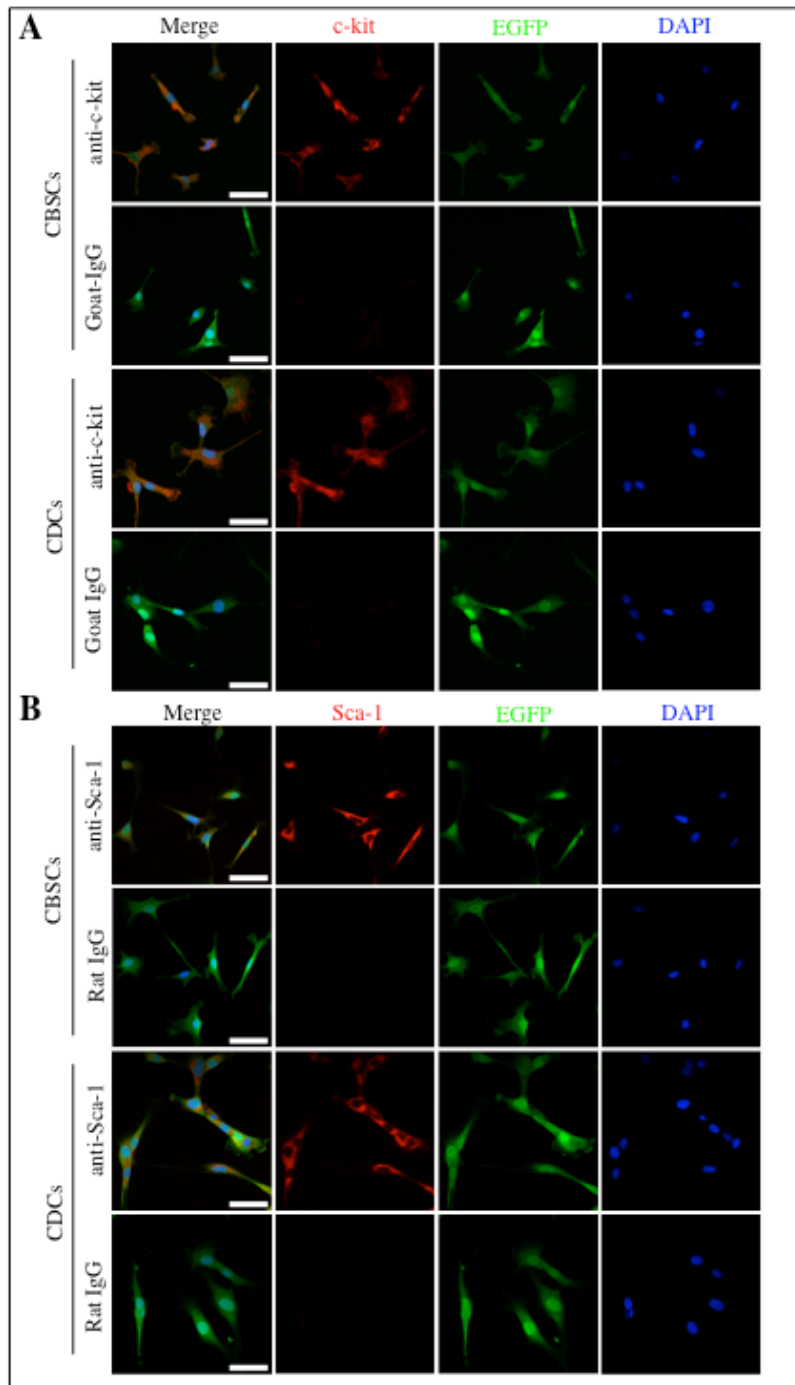


*Figure 2: Characterization of stem cells by immunostaining.* CBSCs or CDCs were stained for A) c-kit or B) Sca-1 (red) and nuclei were labeled with DAPI (blue). Isotype controls area also shown (goat IgG for c-kit or rat IgG for Sca-1). Scale bars = 50 um.

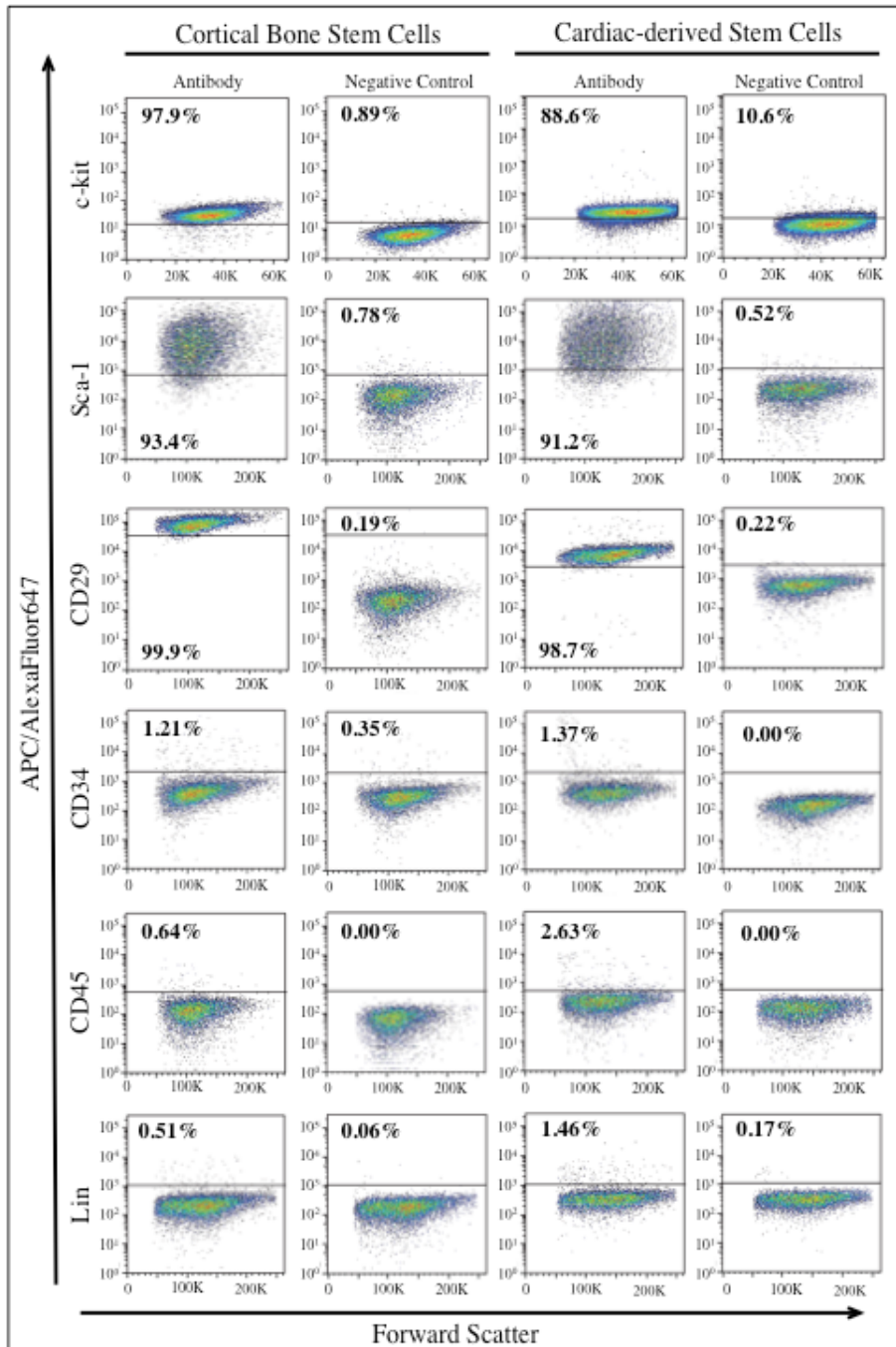


**Figure 3: Characterization of cortical bone stem cells using flow cytometry.** Flow cytometry against c-kit, Sca-1, CD29, CD34, CD45 and lineage markers (Lin). Results are shown along with negative isotype controls in which cells were labeled only with APC-conjugated Rat IgG2A.

mRNA in stem cells are shown in Figure 1. CBSCs expressed greater levels of both transcripts than did CDCs: over 3-fold higher levels of c-kit and 2-fold higher levels of Sca-1. Both stem cells types demonstrated positive membrane immunostaining for c-kit and Sca-1 (Figure 2). Flow cytometry analysis (Figure 3) demonstrated that the majority of CBSCs and CDCs expressed c-kit (CD117), Sca-1, and  $\beta_1$ -Integrin (CD29). Additionally both cell types lacked expression of the hematopoietic stem cell marker CD34, the common leukocyte antigen CD45, and other common markers of the hematopoietic lineage that can be detected by a cocktail of antibodies (Lin) against CD5, CD11b, CD45R, anti-7-4, Anti-Gr-1, Ly6G/C, and Anti-Terr-119.

#### In Vitro Expression of Paracrine Factors

We next studied if the stem cells expressed or secreted paracrine factors that are thought to be involved in cardioprotection, neovascularization, or recruitment of endogenous cardiac stem cells.<sup>48, 72, 73</sup> Eight specific factors produced by CBSCs and CDCs were analyzed: angiopoietin-1 (Ang-1), basic fibroblast growth factor (bFGF), hepatocyte growth factor (HGF), insulin-like growth factor-1 (IGF-1), platelet-derived growth factor (PDGF), stem cell factor (SCF), stromal-derived factor-1 (SDF-1), and vascular-endothelial growth factor (VEGF). HGF and IGF-1 are thought to be cardioprotective: HGF has cytoprotective, antiapoptotic and proangiogenic effects,<sup>73-75</sup> while IGF-1 can inhibit apoptosis and may stimulate growth and proliferation of stem cells.<sup>48, 73, 75</sup>

SCF, and SDF-1 are thought to stimulate stem cell function: SCF, the ligand for the c-kit receptor,<sup>76</sup> may stimulate stem cell homing,<sup>77</sup> while SDF-1 is a chemotactic ligand that induces stem cell proliferation and homing to the site of injury.<sup>48, 72, 73</sup> Ang-1, bFGF, PDGF and VEGF all promote angiogenesis: Ang-1 induces vascular cell migration and enhances stability of newly-formed vasculature,<sup>73, 77</sup> bFGF induces proliferation of endothelial and smooth muscle cells,<sup>48, 73, 75, 77, 78</sup> PDGF stimulates smooth muscle cell proliferation,<sup>48, 73, 77</sup> and VEGF induces endothelial cell proliferation and tube formation.<sup>48, 72, 73, 75, 77, 78</sup> Protein expression of all eight factors was detected by Western analysis performed on CBSC or CDC lysates collected *in vitro* (Figure 4A). Positive expression of these factors *in vitro* was confirmed by immunostaining (Figure 4B). Enzyme-linked immunosorbent assays of stem cell-conditioned media demonstrated that IGF-1, VEGF, and SDF1 were all secreted by proliferating CBSC and CDCs in culture (Figure 4C), and no significant difference between the amount of paracrine factors secreted by each cell type could be detected. Neither HGF nor SCF were secreted in detectable amounts by either stem cell type, even though both factors were seen at the protein level by both Western analysis and immunostaining. These results show that both CBSCs and CDCs *in vitro* produce factors known to be associated with beneficial cardiac remodeling after MI.<sup>48, 74, 75</sup>

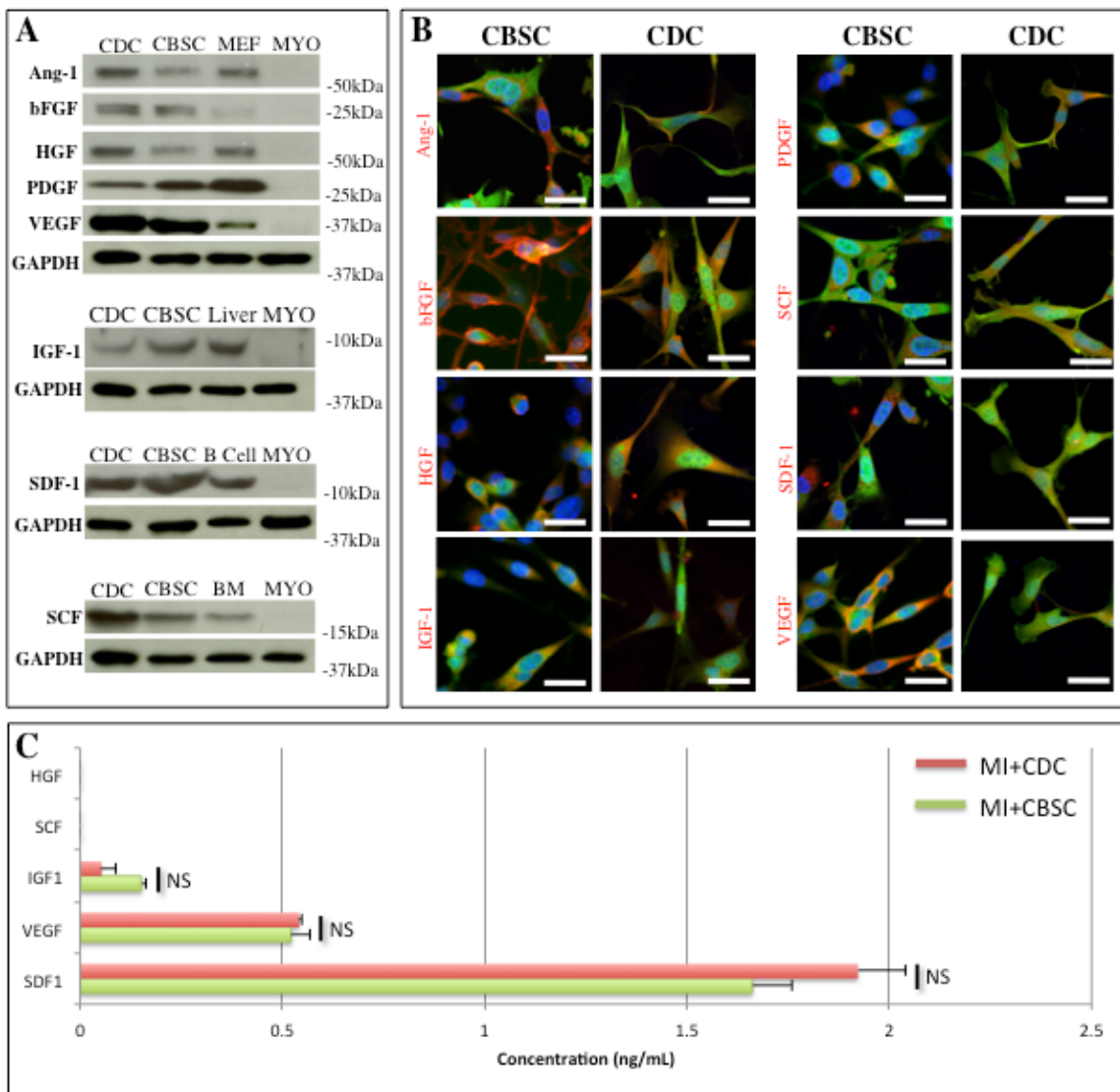


**Figure 4: In vitro characterization of stem cells.** A) CBSC or CDC lysates were analyzed by Western analysis. Positive controls include mouse endothelial fibroblasts (MEF), liver, bone marrow (BM), and B lymphocytes (B Cells). Myocyte (MYO) lysates were used as negative controls for all samples. B) CBSCs (green) were fixed *in vitro* and immunostained against each paracrine factor (red). Nuclei are labeled with DAPI (blue) and scale bars = 20  $\mu$ m. C) CBSCs or CDCs were allowed to proliferate over 72 hours and their culture

media was analyzed by ELISA for the presence of soluble HGF, IGF, SCF, SDF1, and VEGF. Samples were analyzed in triplicate and background signal was subtracted using unconditioned media blanks. NS = No Significant difference.

**CBSCs differentiate in vitro in co-culture with neonatal rat ventricular myocytes**

Both bone marrow-derived<sup>56, 67</sup> and cardiac-derived stem cells<sup>79</sup> have previously been described to differentiate *in vitro* in co-culture with neonatal rat ventricular myocytes. When EGFP+ CBSCs were plated in co-culture with neonatal rat myocytes to induce differentiation, a small fraction of EGFP+ cells were observed to beat after 72 hours in co-culture, but this occurred only infrequently. To quantify the rate of *in vitro* differentiation, cells were fixed and stained for α-sarcomeric actin (Figure 5A) or connexin43 (Figure 5B). Only  $11.5 \pm 0.9\%$  ( $n=5$ ) of EGFP+ cells expressed α-sarcomeric actin and  $7.5 \pm 1.7\%$  ( $n=5$ ) appeared coupled via connexin43 gap junctions to their neighboring cells. Thus, like bone-marrow or cardiac-derived stem cells, CBSCs demonstrate some capacity to differentiate *in vitro*.

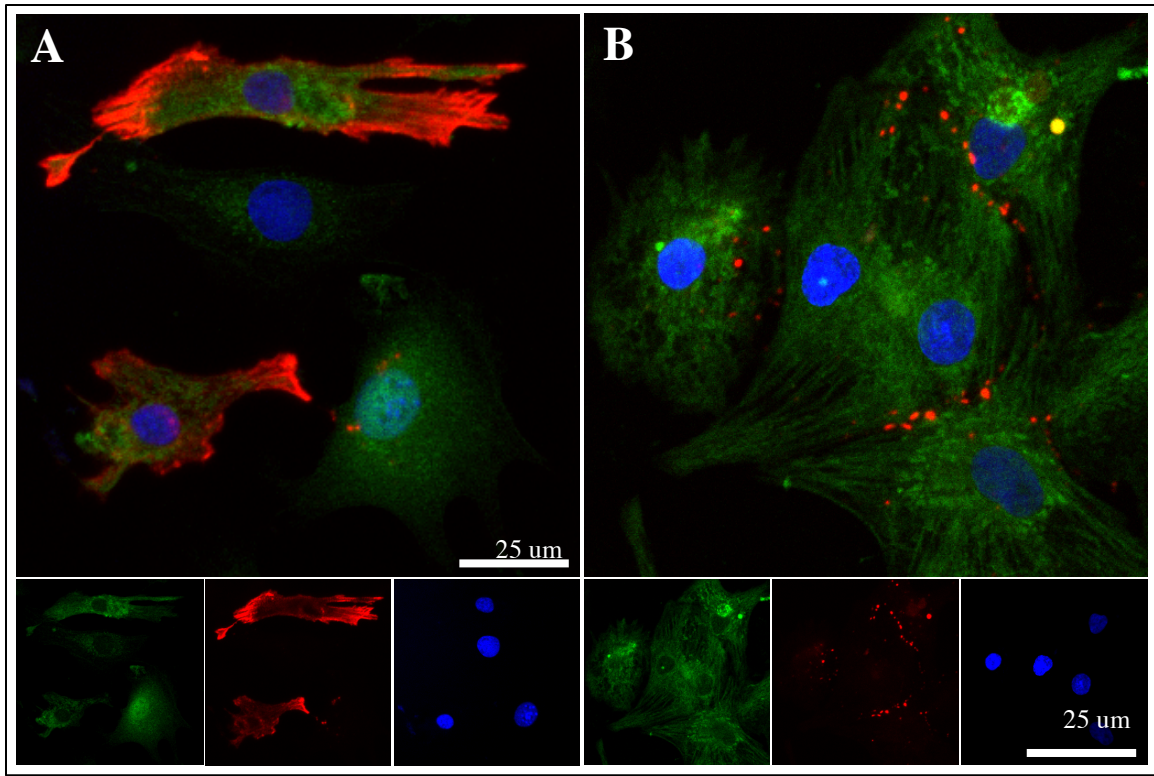


**Figure 5: Bone-derived stem cells differentiate in vitro.** EGFP+ CBSCs (green) were cocultured with neonatal rat ventricular myocytes for 3 days. Cells were fixed and stained for **A**)  $\alpha$ -sarcomeric actin or **B**) connexin43 (red). Nuclei are labeled with DAPI (blue).

## CHAPTER 4: STEM CELLS SUPPORT THE INJURED HEART *IN VIVO*

CBSC transplants improved survival and cardiac function, attenuated adverse left ventricular remodeling and reduced infarct size

The effects of CBSCs versus CDCs on post-MI structural and functional remodeling were studied. The MI procedure reduced 6-week survival to 50.4% in animals receiving sham saline injections. Animals receiving MI and CBSC therapy demonstrated a 76.5% 6-week survival, which was significantly greater than the saline-treated controls or CDC-treated animals (Figure 6). Animals

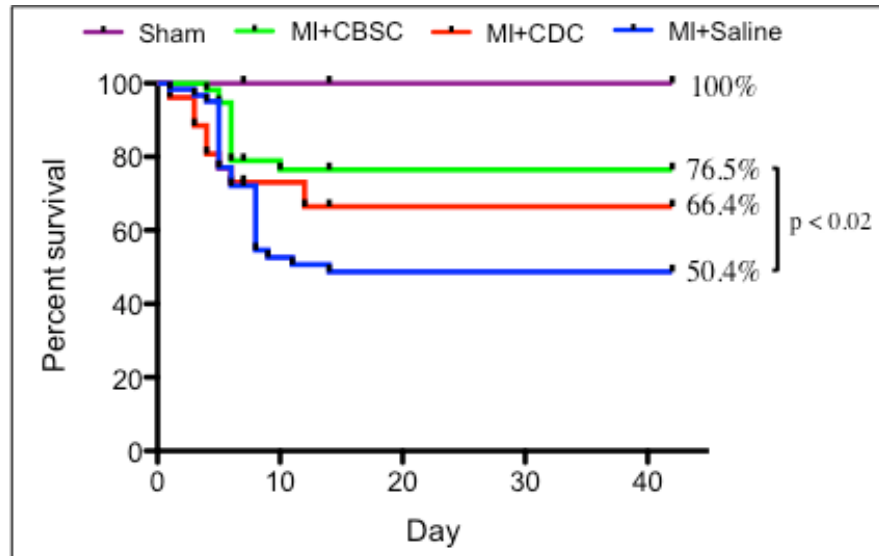
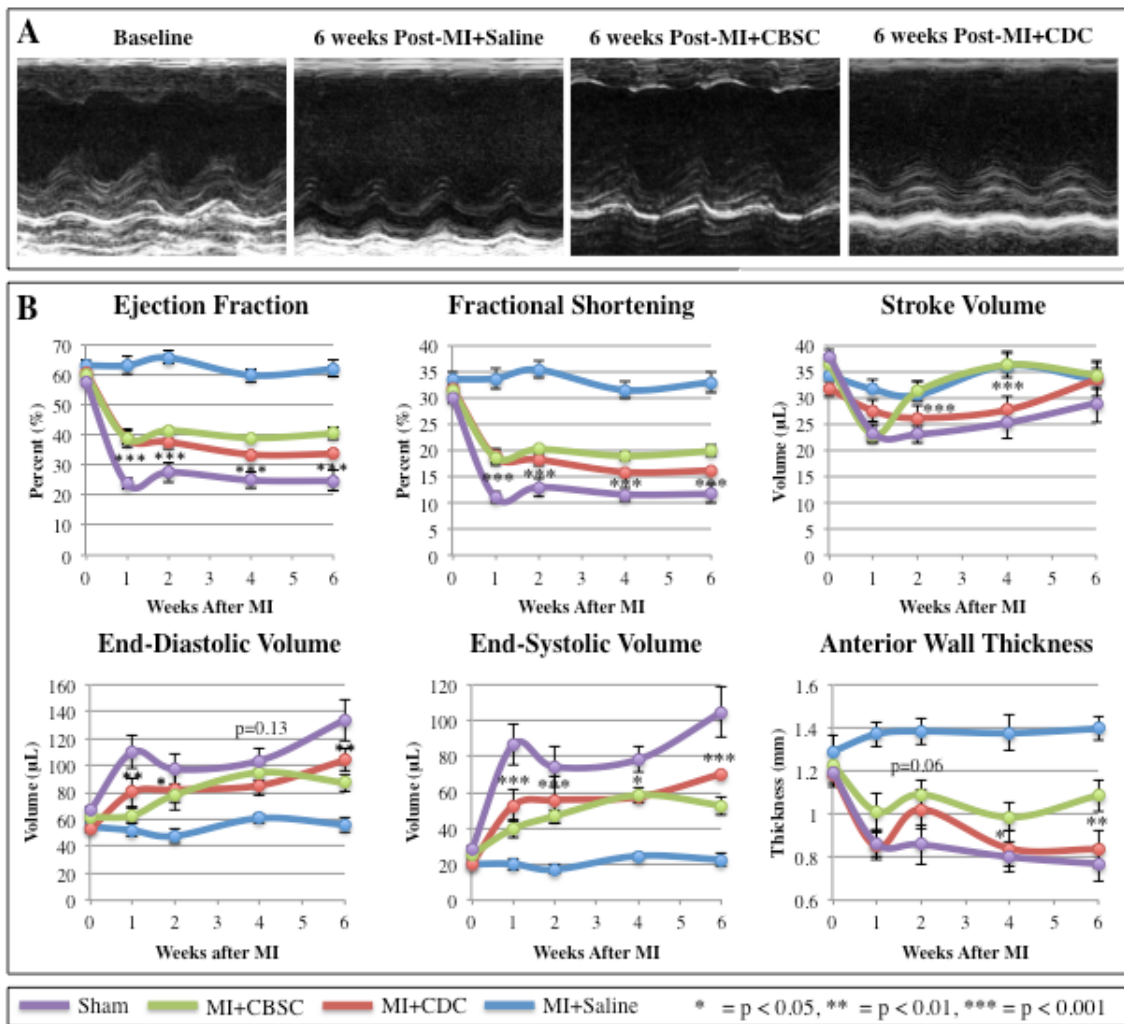


Figure 6: 6 week survival. Mice underwent sham, MI+Saline, MI+CDC or MI+CBSC surgery. Data was analyzed using a Kaplan-Meier regression and significance was determined using the Log-Rank test.

receiving CDC therapy did demonstrate a smaller improvement in survival relative to saline-treated MI controls (66.4%) but this improvement was not statistically significant. Both stem cell therapies improved cardiac function and attenuated adverse cardiac remodeling characteristic of MIs in this model system (Figure 7), and these changes were most pronounced in the MI+CBSC group. Animals receiving MI+CBSC had significantly improved ejection fraction and fractional shortening compared to the MI+Saline control animals as early as 1 week post-MI, and these changes were sustained through 6 weeks post-MI. Improvements in ejection fraction and fractional shortening were greater among CBSC treated animals than CDC treated animals. Both stem cell treatment groups experienced an initial decline in stroke volume (SV), but SV returned to normal by 2 weeks post-MI and remained significantly improved relative to MI+Saline control animals. Animals in the MI+Saline group demonstrated significant increases in end-diastolic and systolic volumes with thinning of the infarct-affected anterior wall (Figure 7). By contrast, MI animals treated with CBSCs or CDCs had significantly smaller post-MI diastolic and systolic volumes at all time points studied, and they demonstrated attenuated thinning of the anterior wall relative to saline-injected controls, with CBSC treated animals demonstrating the most profound attenuation across all parameters (Figure 7).



**Figure 7: Cardiac function measured by echocardiography.** Animals underwent sham, MI+Saline, MI+CBSC or MI+CDC surgeries and received follow-up serial echocardiography at 1, 2, 4 and 6 weeks post-MI. A) Representative M-mode tracings from animals at baseline, 6 weeks post-MI+Saline, 6 weeks post-MI+CBSC or 6 weeks post-MI+CDC. B) Structural and functional parameters derived from echocardiography measurements are shown.

Five mice were randomly selected from each group (MI+Saline, MI+CDC, or MI+CBSC) to undergo acute infarct size analysis at 24 hours post-MI, and no significant difference between the area at risk (AAR) or ischemic area (IA) was detected between animals in any group (Figure 8). These results demonstrate that acute infarct size was similar in all study animals. Therefore, the structural and functional improvements in the MI+CBSC and MI+CDC groups can be attributed to the effects of cell transplantation alone and are not the result of a stem cell mediated reduction in initial infarct size.

After 6 weeks post-MI, chronic infarct size was analyzed by measuring the area of infarcted tissues relative to total myocardial area on hematoxylin and eosin (H&E)-stained cross sections from saline-, CDC-, or CBSC-injected hearts. Animals receiving either CDC or CBSC therapy had significantly smaller infarcted areas relative to saline-treated controls, with CBSC-treated animals demonstrating the most significantly reduced infarct sizes, suggesting that infarct size or expansion were reduced 6 weeks after CBSC therapy.

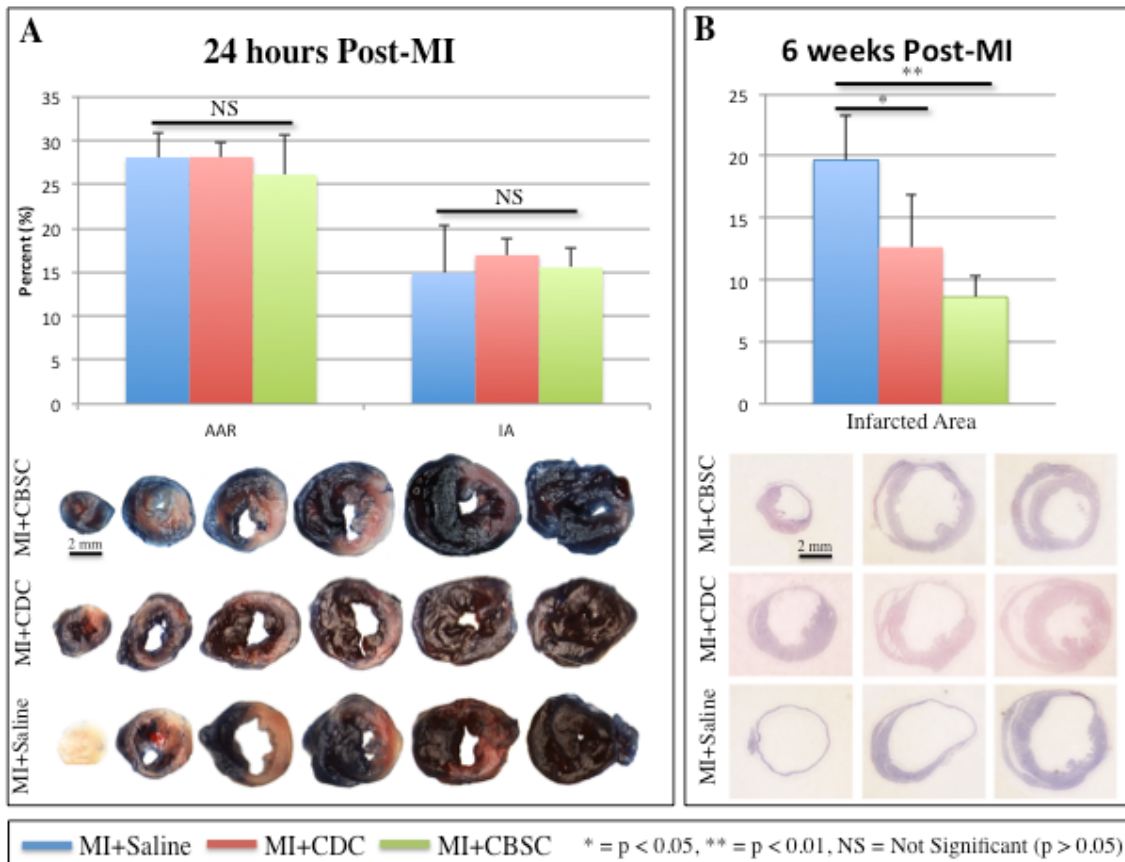


**Figure 8: Infarct size analysis.** **A)** Acute infarct size analysis was performed on animals receiving MI+Saline (n=5), MI+CDC (n=5), or MI+CBSC (n=5) that were sacrificed 24 hours post-MI. Their area at risk (AAR) or infarct area (IA) was determined using Evan's Blue or triphenyltetrazolium chloride staining, respectively, and results are reported as a percentage of total ventricular area. **B)** Chronic infarct size was determined by staining short-axis cross-sections from hearts fixed at 6 weeks post-MI+Saline (n=6), MI+CDC (n=6), or MI+CBSC (n=5) with hematoxylin and eosin (H&E) and measuring the infarct area as a percent of total myocardial surface area.

Contractile myocardium was detected at CBSC injection sites

Strain analysis was performed on long-axis B-mode images to determine if regions injected with CBSCs developed contractile activity. Figure 9A shows representative three-dimensional wall velocity diagrams for 3 consecutive cardiac cycles taken from animals at baseline, 6 weeks post-MI+Saline, and 6 weeks post-MI+CBSC. Supplemental Figure 10 outlines how 3D wall velocity diagrams are constructed relative to the acquired parasternal long-axis B-mode echocardiogram of the left ventricle. Points along the left ventricular (LV) endocardial surface are plotted along the x-axis, from the base of the posterior wall to the apex to the base of the anterior wall. At baseline, the hearts demonstrated even and synchronous contraction and relaxation across the LV endocardium (Figure 9A). In the MI+Saline control group after 6 weeks, there was a dramatic reduction in wall velocity across the endocardium of the infarct-related anterior wall (Figure 9A). CDC-treated animals demonstrated some improvements in wall velocity at the infarct border zone, while CBSC-treated MI animals demonstrated even greater improvements in wall velocity at the infarct border zone segments where CBSCs were injected (Figure 9A).

Figure 9B shows vector diagrams taken from long-axis B-mode echocardiograms. The normal hearts demonstrate even, synchronous contractions and relaxations throughout the cardiac cycle. Animals with MI injury showed pronounced LV chamber dilation, wall thinning, and hypokinesis of the infarcted wall, as evidenced by the lack of vector activity in this region. In animals receiving stem cell therapy, the LV chamber was less dilated, and there

was attenuated wall thinning and increased contractile activity in the border zone segments that received cell therapy. While CDC-treated animals did show some improvements in wall velocity and strain at the border zone segments, CBSC-treated animals generated much greater wall velocities and contraction vectors nearly equal in magnitude to baseline control hearts at the infarct border zone segments where CBSCs were injected.

Global averages of LV endocardial strain and strain rate are plotted in Figure 9C. Strain, which measures change in length relative to the initial length ( $\text{Strain} = \text{Final Length } [L]/\text{Initial Length } [L_0]$ ) was measured either in the radial (from the center of the ventricle cavity outward) or longitudinal axis (from the apex to the base). The rate of change in strain (Strain Rate = Strain/Time) was also calculated. In both axes, strain and strain rate were significantly reduced following MI. Significant improvements in both strain and strain rate in both the radial and longitudinal axes were observed in MI animals receiving CBSC or CDC therapy relative to MI+Saline controls, and CBSC-treated animals showed improved strain relative to CDC animals across all parameters at all time points. These data demonstrate that CBSC-treated hearts showed significantly improved global and regional contractility by 6 weeks after an MI.

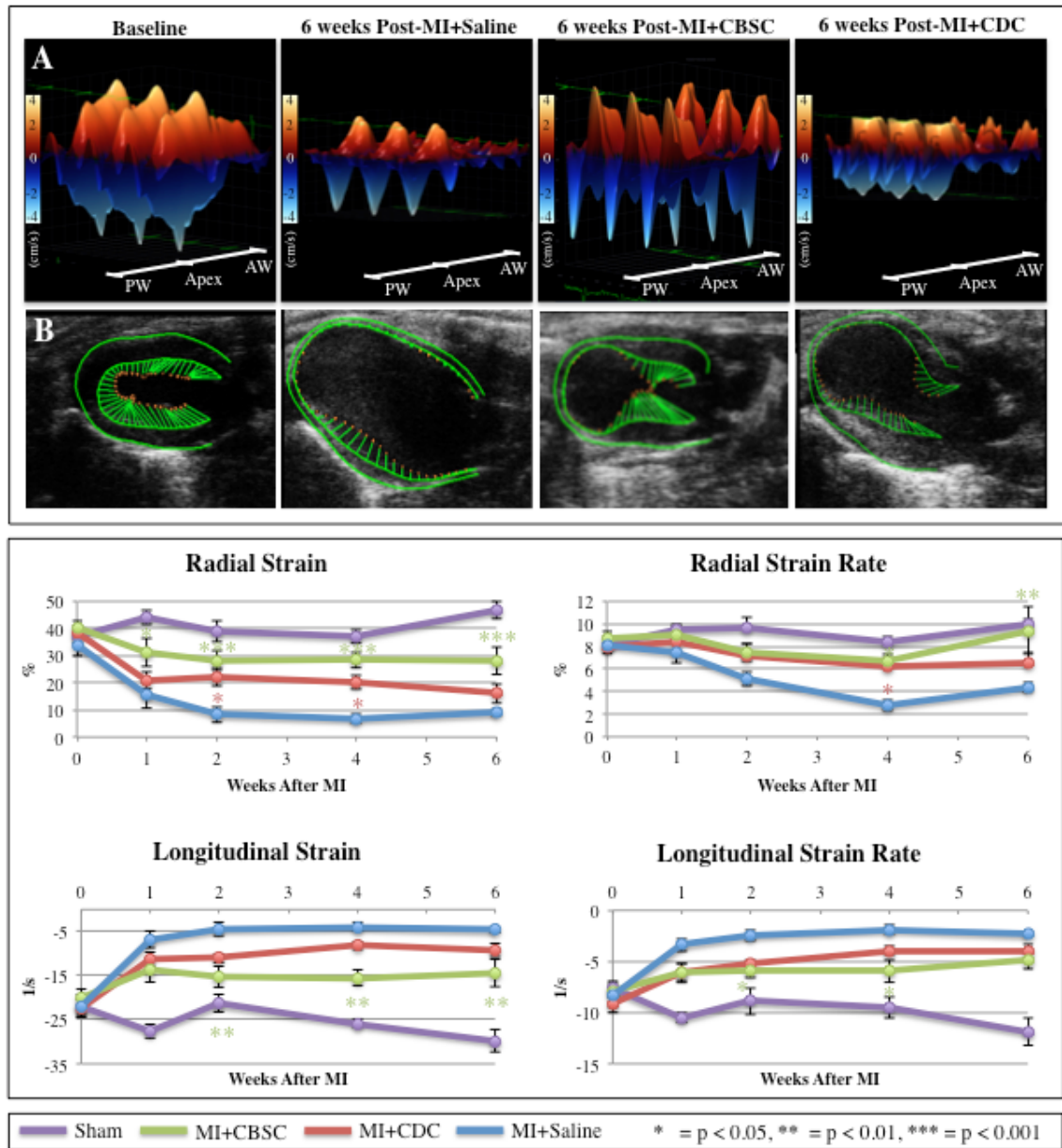


**Figure 9: Left ventricular endomyocardial strain.** A) Three-dimensional regional wall velocity diagrams showing contraction (orange/positive values) or relaxation (blue/negative values) of 3 consecutive cardiac cycles. B) Vector diagrams showing the direction and magnitude of endocardial contraction. C) Global averages of strain and strain rate measured in the radial or longitudinal axes across the LV endocardium.

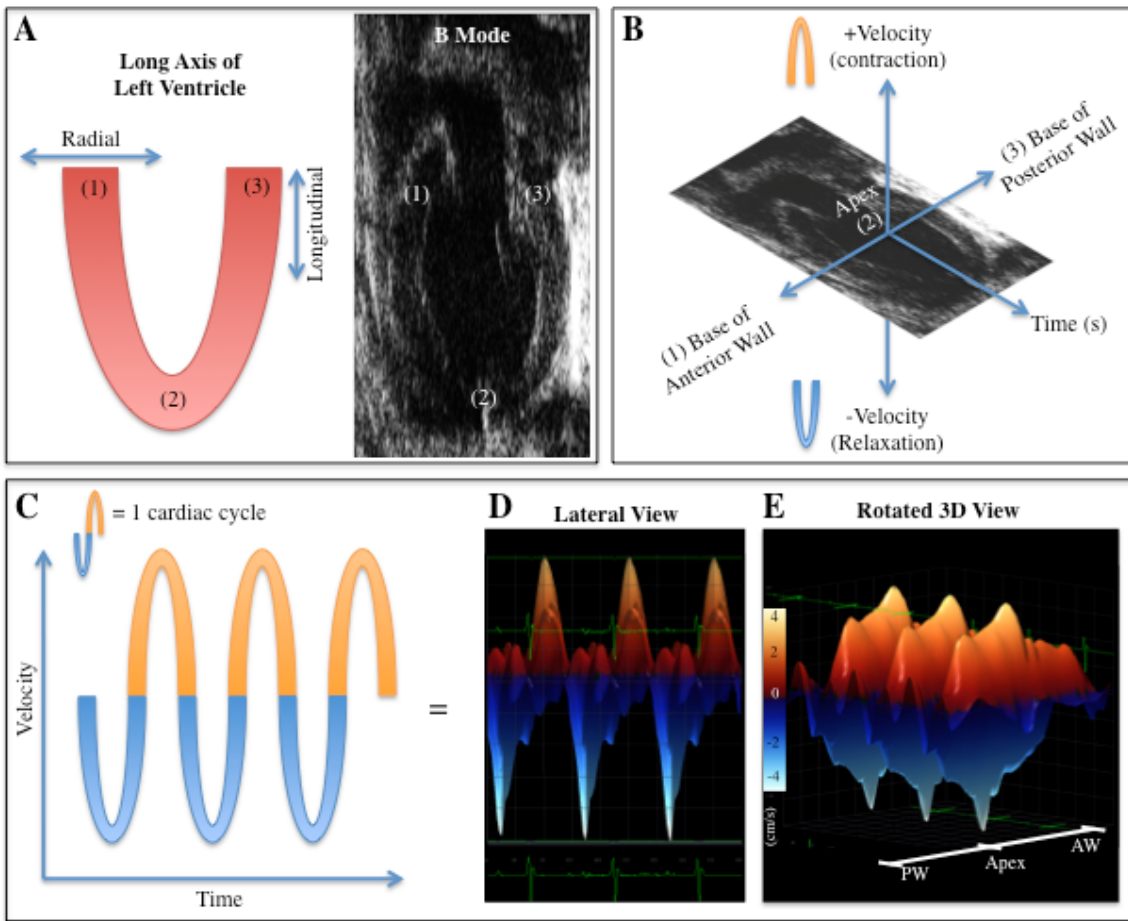


*Figure 10: Diagram of strain analysis measurements.* **A)** Schematic showing the measurement parameters used for strain analysis on B-mode images taken in the parasternal long axis. A sample B-mode tracing of a mouse heart at baseline is included at right. **B)** Diagram explaining the three axes used to generate the 3D wall velocity diagrams. The X-axis represents the location along the LV endocardial surface from the base of the anterior wall (1) to the apex (2) to the base of the posterior wall (3). The Z-axis represents time (in seconds), which is measured off of the electrocardiogram. The Y-axis represents contraction (positive values or orange color) or relaxation (negative values or blue color). An example of a positive wall velocity tracing (orange) and a negative velocity

tracing (blue) are shown next to the positive and negative Y-axes. **C)** Diagram demonstrating how the 3D wall velocity diagram is constructed. A single cardiac cycle is shown (one blue and one orange tracing), and below a cartoon illustrating 3 consecutive cardiac cycles is shown. This is equivalent to what is seen in the lateral view of the wall velocity diagram (**D**). **E)** Shows the rotated view of the 3D wall velocity diagram from the animal at baseline that was shown in Figure 9.

## **CHAPTER 6: EVIDENCE OF PARACRINE FACTOR SECRETION BY STEM CELLS *IN VIVO***

*Expression of pro-angiogenic paracrine factors in vivo by stem cells induces new blood vessel formation*

The environment in the infarct border zone is dramatically different from that in the tissue culture dish. Therefore, paracrine factor expression and production are likely to change after transplantation of CBSCs into the infarcted heart. At 24 hours post-MI, hearts receiving CBSC transplants were immunostained for the 8 paracrine factors studied *in vitro*. Injection sites containing EGFP+ CBSCs were identified and found to express bFGF and VEGF, but Ang-1, IGF-1, HGF, or PDGF were not found at any injection sites examined (Figure 11). Injection sites containing EGFP+ CDCs were found to express Ang-1 in addition to bFGF and VEGF, but they were likewise negative for all 5 of the other factors. These studies suggest that, when injected into the MI border zone, CBSCs express only bFGF and VEGF (and CDCs express only Ang-1, bFGF, and VEGF). Despite expressing an additional paracrine factor after 24 hours, expression of all paracrine factors by CDCs was not sustained. No amounts of Ang-1, bFGF, or VEGF could be detected in any CDC injection sites after 24 hours post-MI (data not shown).

In contrast, VEGF expression was detected in CBSC injection sites as late as 2 weeks post-MI. Figure 12 shows expression of VEGF (red) by an engrafted

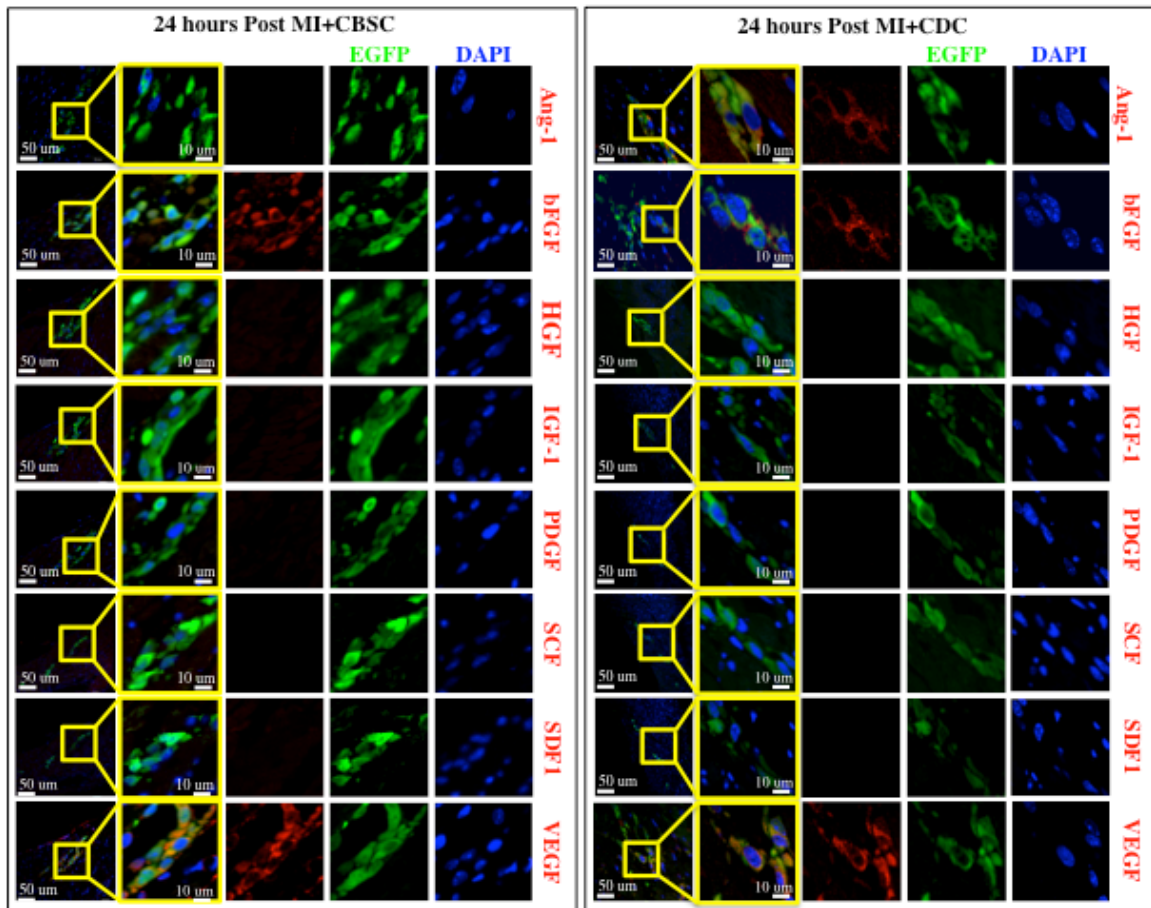


**Figure 11: Characterization of paracrine factors secreted by stem cells after 24 hours post-MI in vivo.** Animals receiving MI+CBSCs were sacrificed 24 hours post-MI for analysis of paracrine factor production. EGFP+ CBSCs stained positive for bFGF, and VEGF (shown in red), but negative for HGF, IGF-1, PDGF, SCF, and SDF-1. EGFP+ CDCs stained positive for Ang-1 in addition to bFGF and VEGF, but also stained negative for HGF, IGF-1, PDGF, SCF, and SDF-1. Nuclei are labeled with DAPI (blue) and injected CBSCs are green.

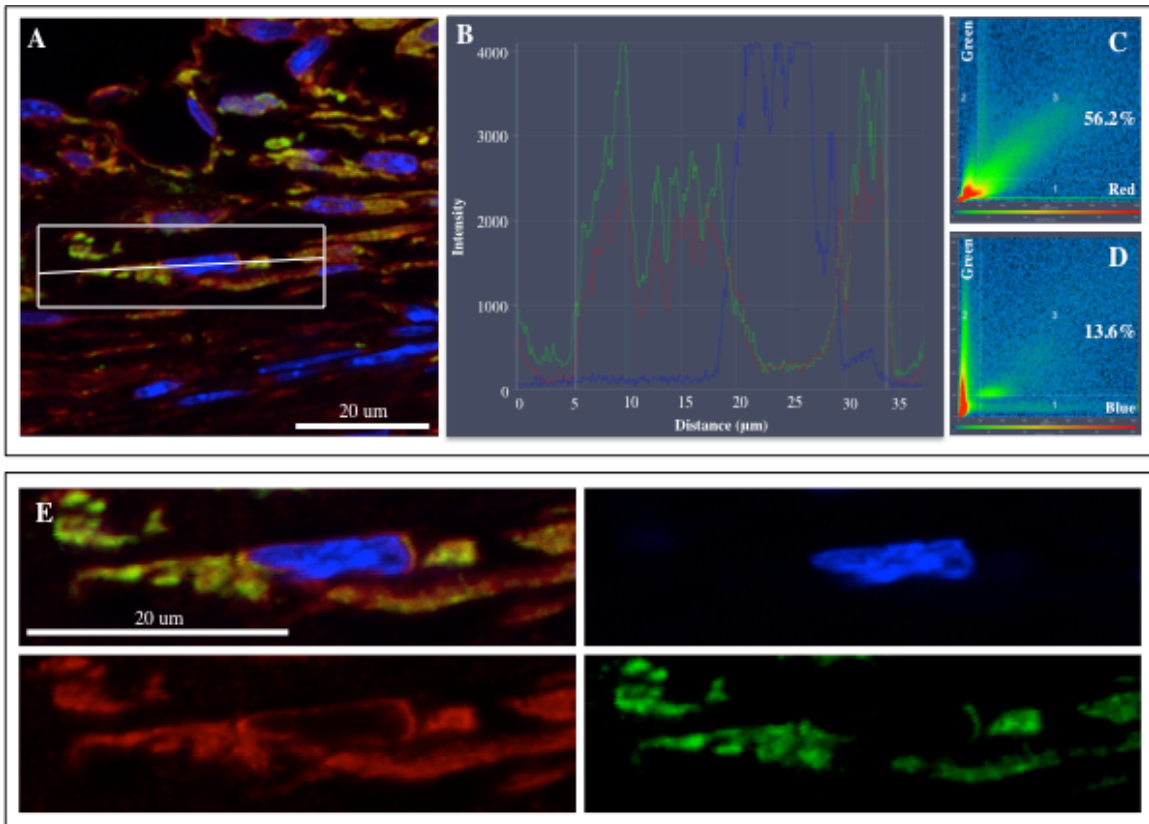


**Figure 12: Characterization of paracrine factors secreted by cortical bone stem cells *in vivo* 2 weeks after MI.** Animals receiving MI+CBSCs were sacrificed 2 weeks post-MI and EGFP+ CBSC injection sites were identified and immunostained for VEGF (red). Nuclei are labeled with DAPI (blue). **A)** Immunostain showing an EGFP+/VEGF+ cell that was selected for fluorophore colocalization analysis by confocal line scan. **B)** Intensity of red, green, and blue phlorophores across the line scan of the cell selected in Figure A. From these data, scatterplots were constructed depicting colocalization of **C)** red vs. green channel or **D)** blue vs. green channel (control). **E)** Magnified image depicting the cell in Figure A along with single color channel images.

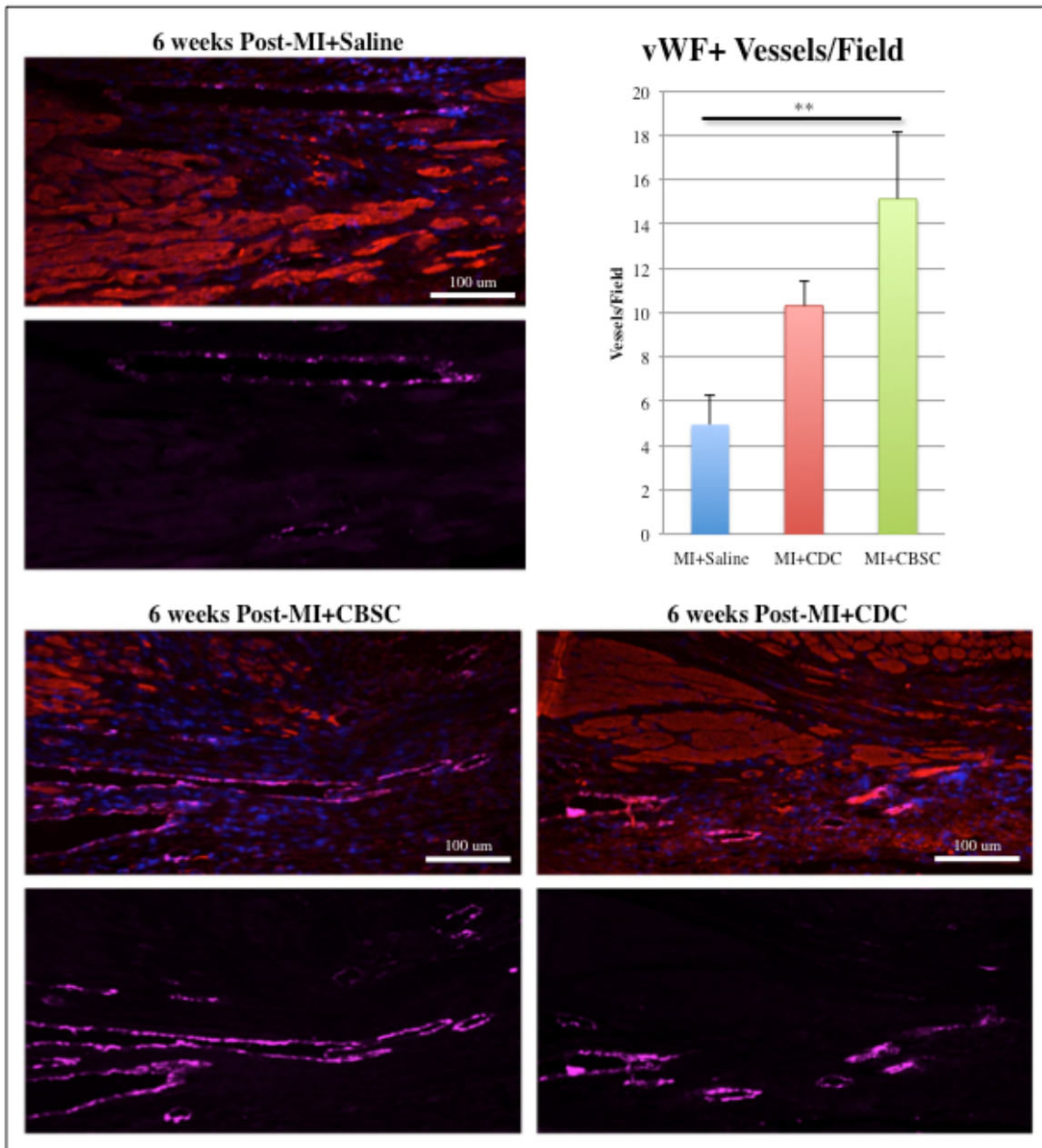


Figure 13: Stem cell-treated animals have increased von Willebrand Factor+ blood vessels near the infarct border zone by 6 weeks post-MI. Slides from animals receiving MI+Saline, MI+CDC or MI+CBSC injection were stained for von Willebrand factor (purple) and  $\alpha$ -sarcomeric actin (red), and the number of

von Willebrand Factor+ blood vessels observed per high-powered field (HPF) were quantified. \*\* = p < 0.001

EGFP+ CBSC at 2 weeks post-MI. Figures S-VIIB shows the fluorescence intensity tracings of each color channel (green = EGFP, red = VEGF, blue = DAPI) across a confocal line scan of the cell selected in Figure 12A that demonstrates the colocalization of the VEGF and EGFP signal. Figure S-VIIC shows a scatterplot of pixel intensities in the red channel versus the green channel, and the diagonal deflection represents colocalized red/green pixels (56.2% of green and red pixels in this line scan were colocalized). Figure 12D shows a control scatterplot of the blue (DAPI) versus green channel (only 13.6% of blue and green pixels were colocalized). Interestingly, paracrine factors involved in homing and recruitment of endogenous stem cells (SCF and SDF-1) were not detected at any time point *in vivo*.

To determine whether the *in vivo* expression of the CBSC-secreted pro-angiogenic factors bFGF and VEGF (and Ang-1 secreted by CDCs) resulted in increased neovascularization, blood vessel density was measured in the infarct zones from MI animals treated with saline, CDCs or CBSCs (Figure 13). MI animals receiving CBSC treatment had  $15.13 \pm 3.04$  von Willebrand factor (vWF)-positive blood vessels (purple) per 20X field of view and MI animals receiving CDC therapy had  $10.13 \pm 1.13$  vWF+ vessels per field, while saline-treated

controls had only  $4.95 \pm 1.30$  vWF+ vessels per field. These data support the idea that secretion of pro-angiogenic paracrine factors *in vivo* by both stem cell types, and especially by CBSCs, induced increased neovascularization. Increased blood supply to the injured heart could have contributed to the functional benefits we observed following CBSC transplant. The majority of these blood vessels did not contain EGFP+ cells, suggesting that they were derived via endogenous repair rather than from the injected cells.

## CHAPTER 7: EVIDENCE OF TRANSDIFFERENTIATION *IN VIVO*

EGFP+ CBSCs expand over time as cells proliferate and CBSCs

transdifferentiate into five distinct phenotypes

CBSC injection sites were examined 1, 2 and 6 weeks after MI (Figure 14). Injection sites were identified after immunostaining against  $\alpha$ -sarcomeric actin (red) and EGFP (green). Histological samples from CBSC- and saline-injected hearts were stained simultaneously, and the absence of EGFP signal in the saline-injected controls was confirmed. All tissue sections were first examined under low magnification to identify injection sites and then high magnification images were analyzed. At 1-week post-MI, the majority of cells were found in discrete groups of small, round, poorly differentiated cells. By 2 weeks post-MI, the area of the heart with EGFP+ cells had expanded and the majority of these EGFP+ cells were larger and had an elongated appearance. By 6 weeks Post-MI, injected stem cells had spread throughout the infarct zone and into the infarct border zone and discrete injection sites were no longer visible. Six weeks after injection, the EGFP+ stem cells were spread throughout the border zone and infarct zone.

Time-related changes in CBSC phenotype were studied. After 1 week, most cells were still small (10-20 um) and round in shape (similar to the morphology of the injected cells), but the majority had begun to produce unorganized cytosolic  $\alpha$ -sarcomeric actin (Figure 15A). A small number of cells that had engrafted in close contact with viable endogenous myocytes began to

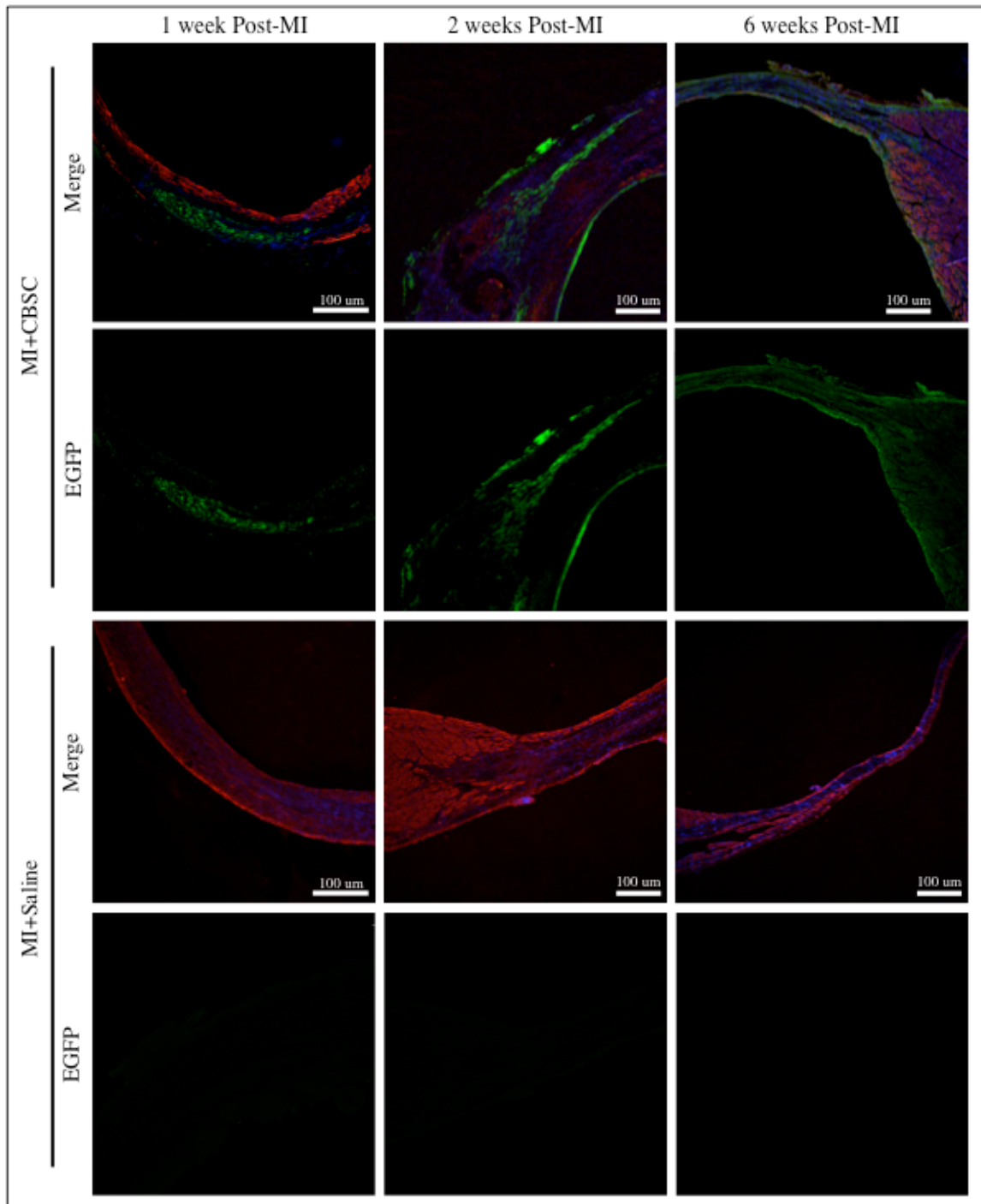


*Figure 14: Expansion of EGFP+ CBSCs as stem cells engraft, align, and elongate over 6 weeks.* Samples were immunostained against  $\alpha$ -sarcomeric actin (red), nuclei are labeled with DAPI (blue) and injected CBSCs are green.

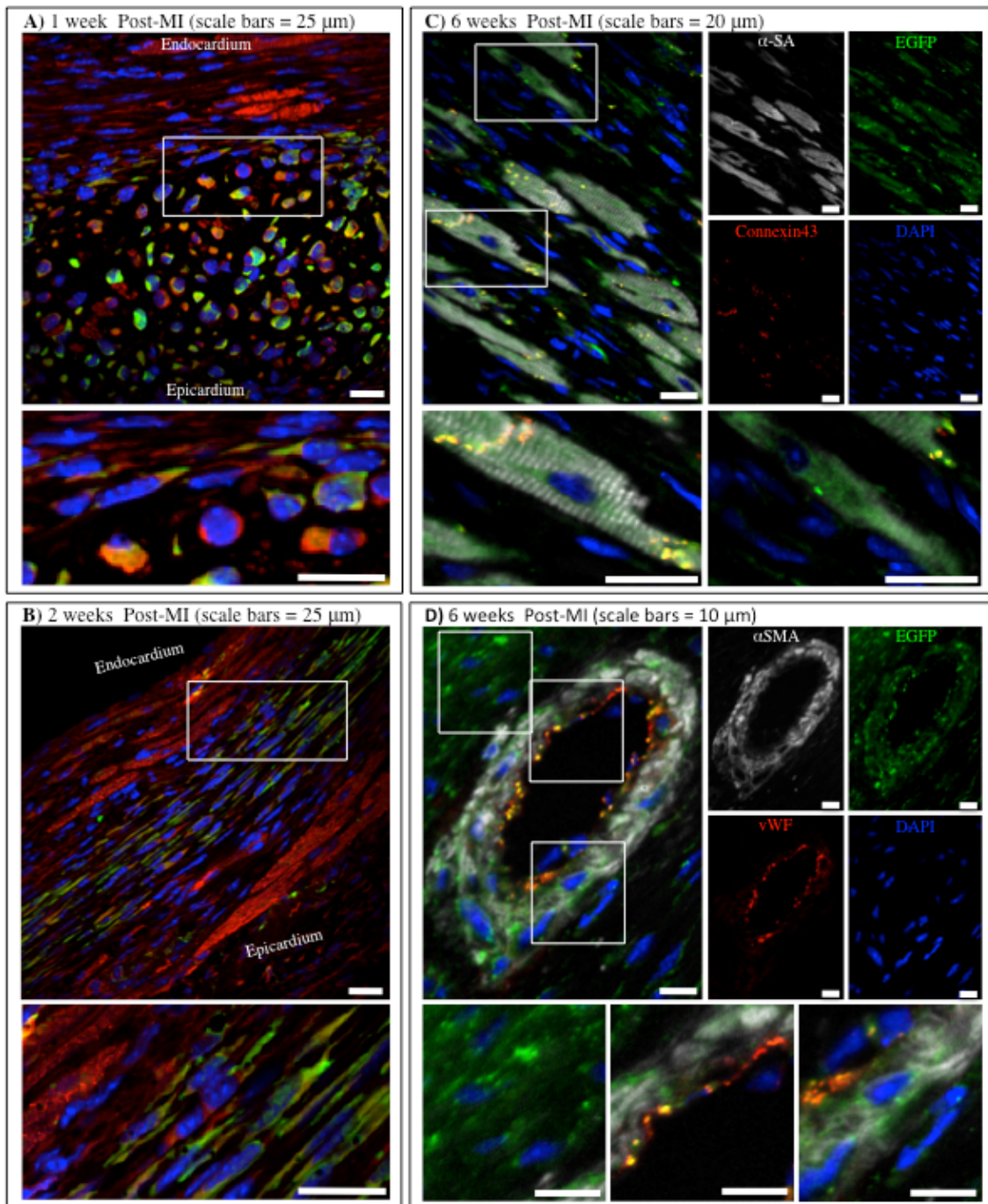


**Figure 15: Stem cells grow and differentiate over 6 weeks.** **A)** 1 week post-MI and **B)** 2 weeks post-MI samples were immunostained for  $\alpha$ -sarcomeric actin (red) and EGFP (green). 6 weeks post-MI samples were immunostained for **C)**  $\alpha$ -sarcomeric actin (white), connexin-43 (red) and EGFP (green) or **D)**  $\alpha$ -smooth

muscle actin (white), von Willebrand Factor (red) and EGFP (green). Nuclei were labeled with DAPI (blue) in all images.

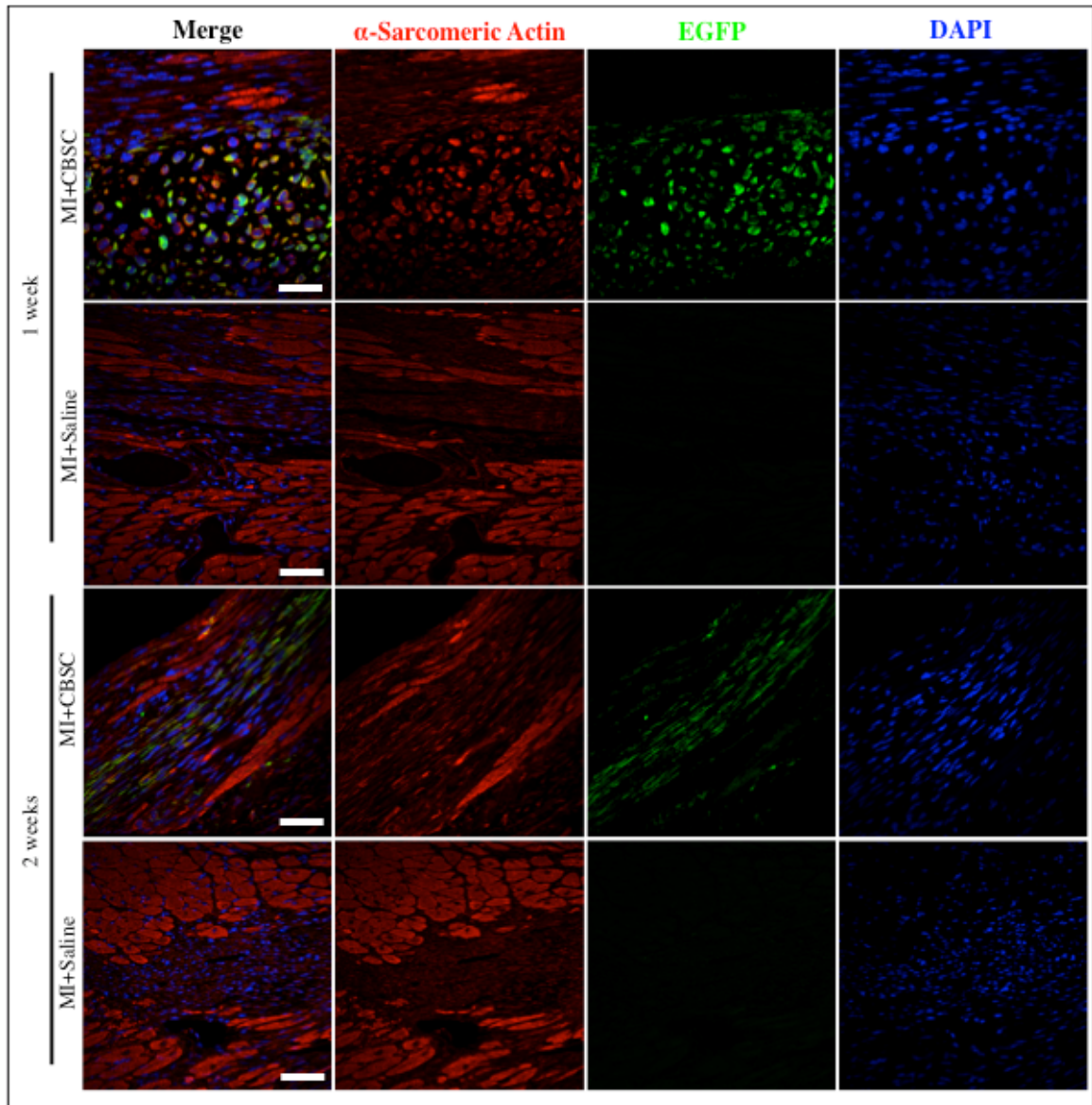


*Figure 16: Individual channel images and staining controls from Figure 7A and B.*

Scale bars = 50 um.

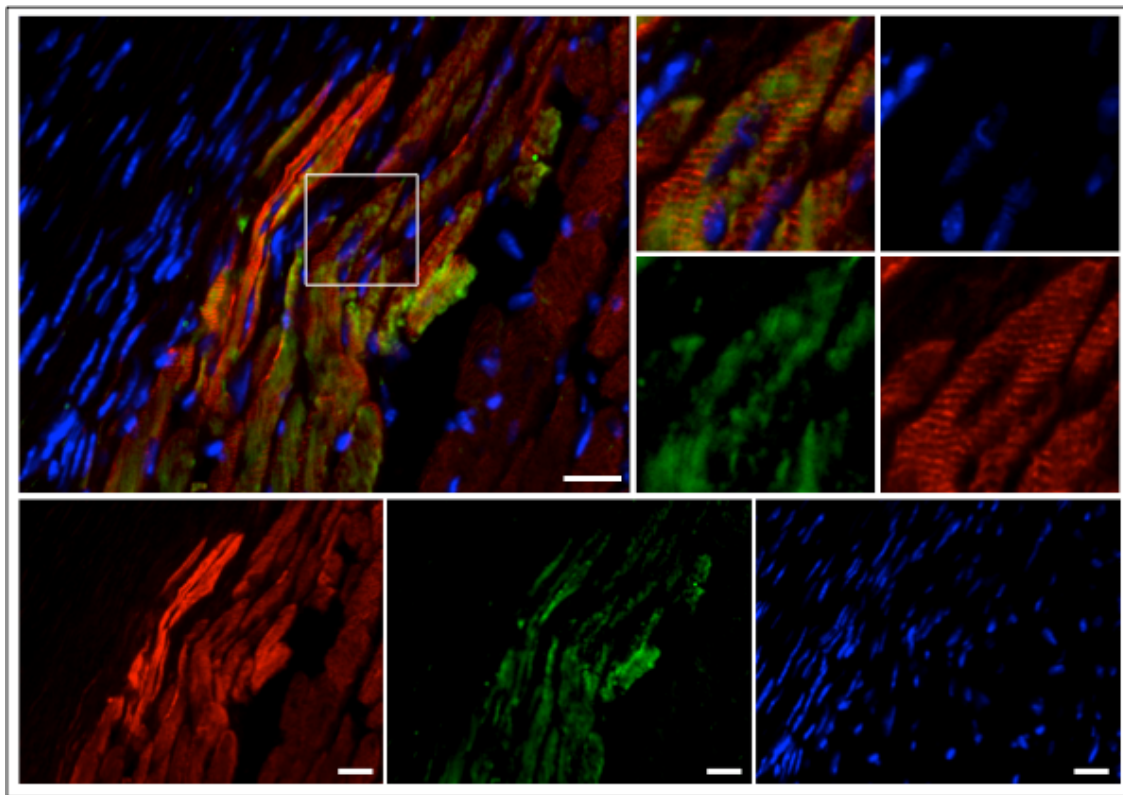


*Figure 17: Low magnification images showing EGFP+ and EGFP- regions of myocardium. Scale bars = 20  $\mu$ m.*

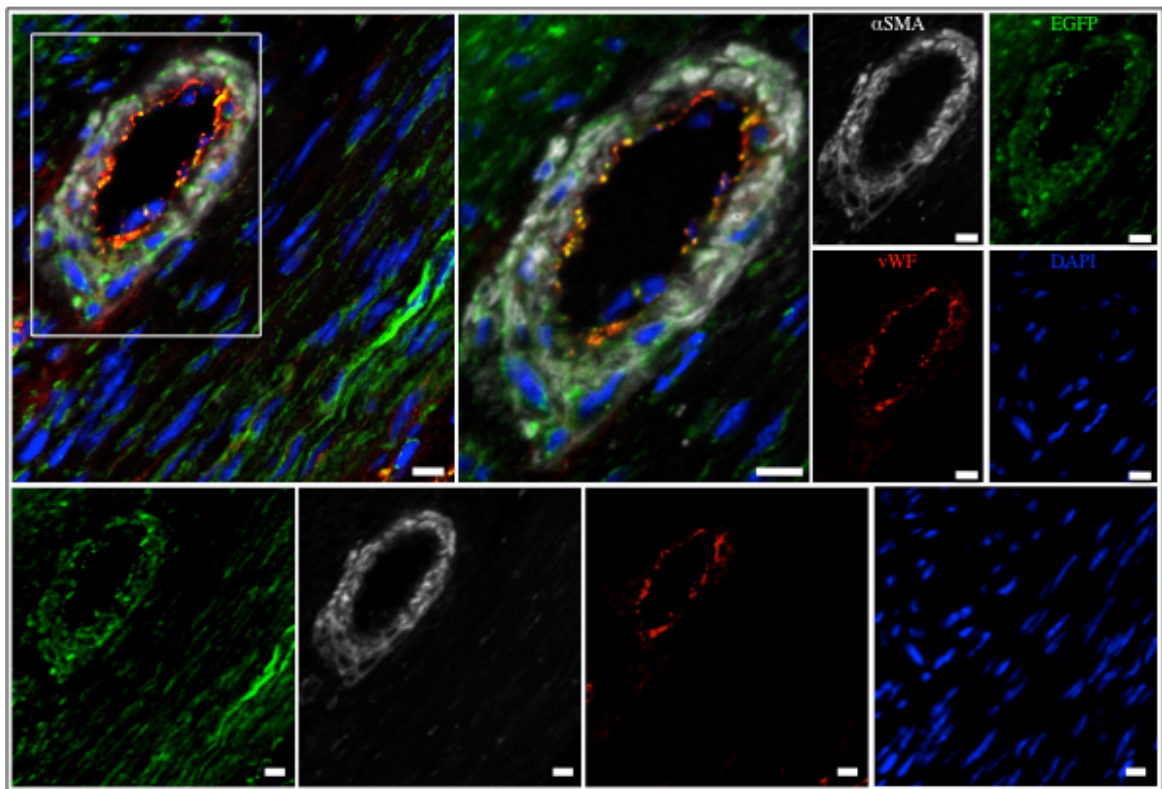


*Figure 18: Low magnification images showing EGFP+ and EGFP- regions around vasculature. Scale bars = 10  $\mu$ m.*

elongate and align in the axis of contraction, as defined by the sarcomeric organization of surviving myocytes in the region. By 2 weeks post-MI, as the injection sites had begun to expand, the majority of cells were elongated, aligned along the axis of contraction, and were expressing additional cytosolic  $\alpha$ -sarcomeric actin (Figure 15B). As at 1 week, cells that had engrafted closest to viable endogenous myocytes appeared the largest and most mature, with even greater amounts of  $\alpha$ -sarcomeric actin visible in their cytoplasm. Although actin expression appeared to be increased by 2 weeks post-MI, it was still relatively unorganized, without the characteristic sarcomeric striations of adult myocytes. Individual color channel images for Figure 15A and B and staining controls for 1 and 2 week post-MI+Saline are shown in Figure 16.

By 6 weeks Post-MI, newly formed EGFP-positive myocardium was visible at the border zone and five distinct EGFP+ stem cell phenotypes were identified: 1) cardiac myocytes that express striated  $\alpha$ -sarcomeric actin and were coupled to neighboring cells via connexin43+ gap-junctions (Figure 15C), 2) cells that express unorganized  $\alpha$ -sarcomeric actin (Figure 15C), 3) vascular smooth muscle cells that stain positive for  $\alpha$ -smooth muscle actin (Figure 15D), 4) vascular endothelial cells that stain positive for von Willebrand factor (Figure 15D), and 5) EGFP+ cells that are smaller (<20 um) and lack any expression of adult cardiomyocyte or vascular cell proteins (Figure 15D). Figure S-17 shows an additional low-magnification image of the CBSC-treated border zone at 6 weeks post-MI in which a newly-formed region of EGFP+ myocardium can be seen adjacent to a region EGFP- endogenous myocardium. Figure 18 shows a

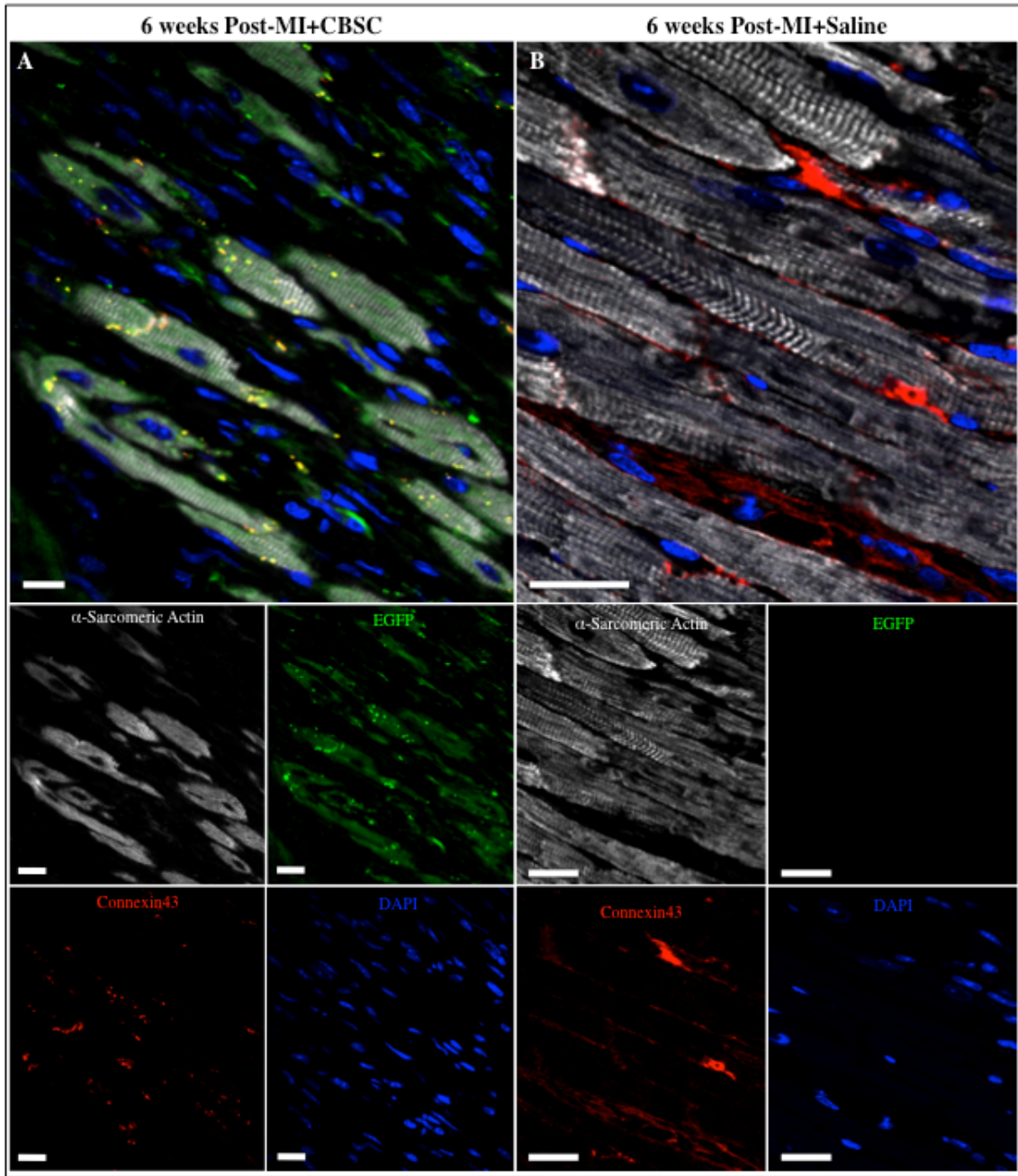


*Figure 19: Individual color channel images and staining controls for Figure 7C.*

Scale bars = 20  $\mu\text{m}$ .

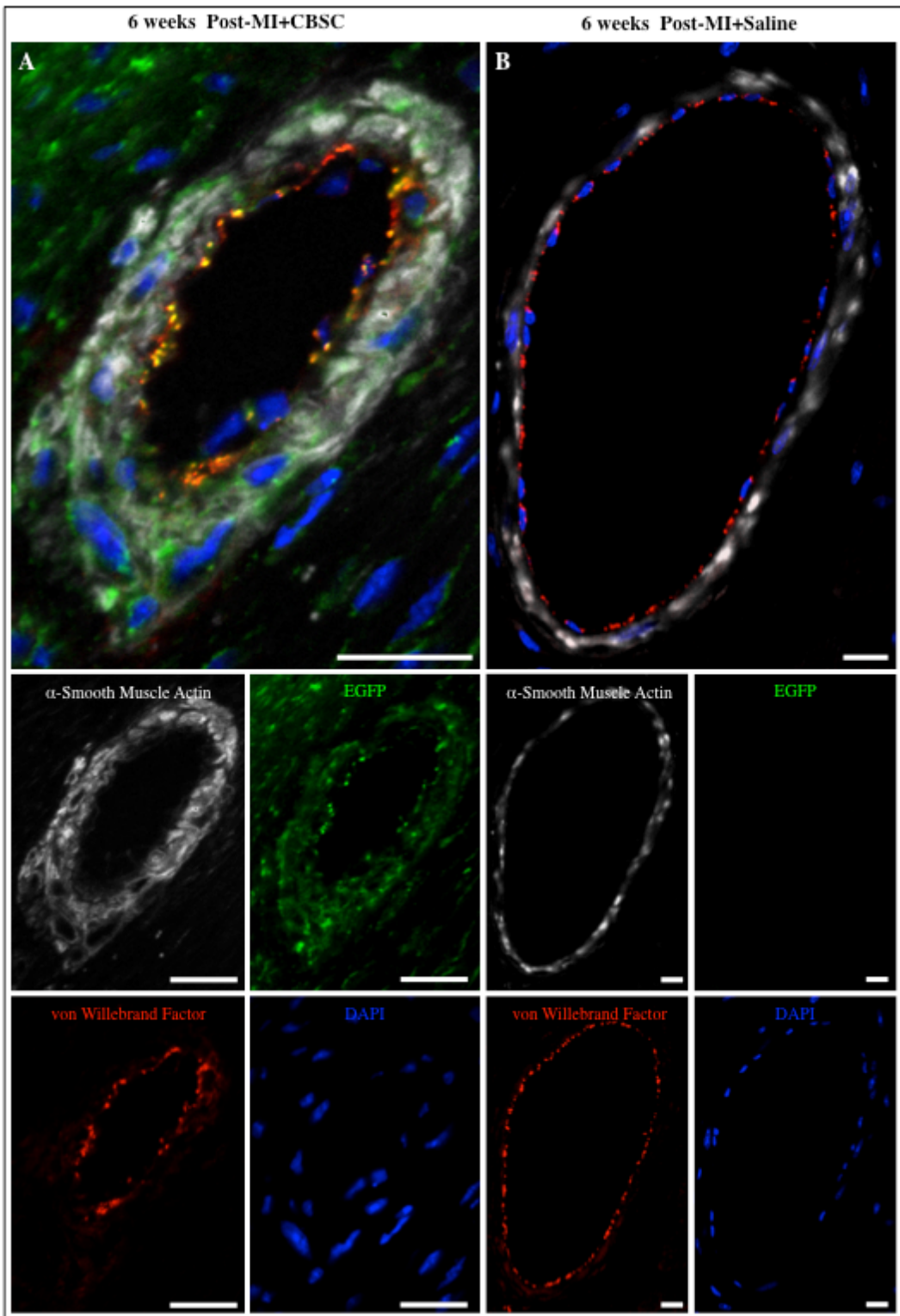


*Figure 20: Individual channel images and staining controls for Figure 7D.*

Vessels from Scale bars = 10 um.

low magnification view of the blood vessel shown in Figure 15D, in which the EGFP+ vessel is clearly surrounded by regions of EGFP- myocardium. Individual color channel images and staining controls for Figure 15C are shown in Figure 19. Individual color channel images and staining controls for Figure 15D are shown in Figure 20. These results support the idea that CBSCs can differentiate into the major cell types of the adult heart.

*Cardiac-derived stem cells expand and proliferate over time but do not adopt an adult myocyte or vascular cell phenotype*

Figure 21 shows images from the hearts of CDC-treated MI animals fixed at 1, 2, and 6 weeks post-MI. EGFP+ CDC injection sites were identified and stained for  $\alpha$ -sarcomeric actin (red) in Figure 21A, or for  $\alpha$ -sarcomeric actin (white) and connexin43 (red) in Figure 21B. Like CBSCs, by 1 week post-MI CDCs initially appear small (10-20  $\mu\text{m}$ ) and round and they have begun to express some unorganized  $\alpha$ -sarcomeric actin. By 2 weeks, the cells have begun to align and elongate like CBSCs and they continue to express unorganized  $\alpha$ -sarcomeric actin. By 6 weeks post-MI, however, no EGFP+ adult cell phenotypes could be identified in CDC-treated animals. Cells continue to grow larger and are still aligned, and some have even begun to express immature connexin43 gap junctions (Figure 21B, right panel), but cytosolic  $\alpha$ -sarcomeric actin is not yet striated and mature gap junctional plaques were not identified. These data suggest that CDCs, unlike CBSCs, did not adopt a cardiomyocyte or vascular phenotype within the 6-week course of this study.

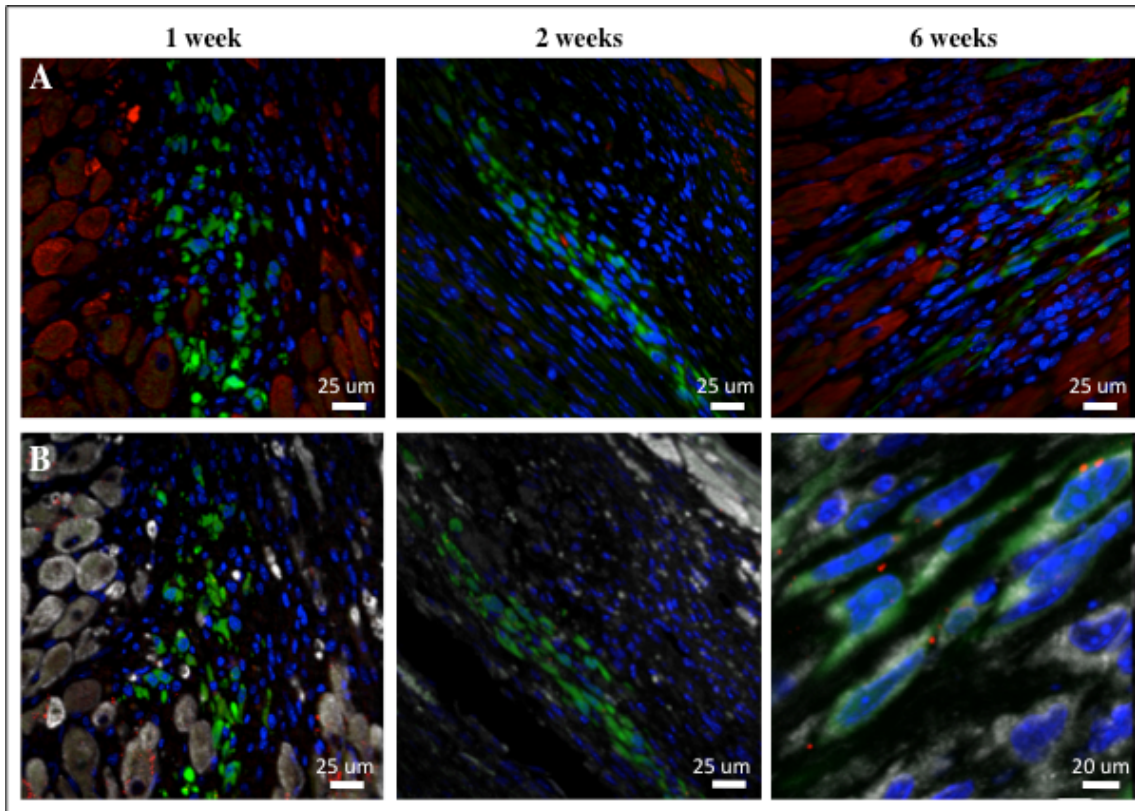
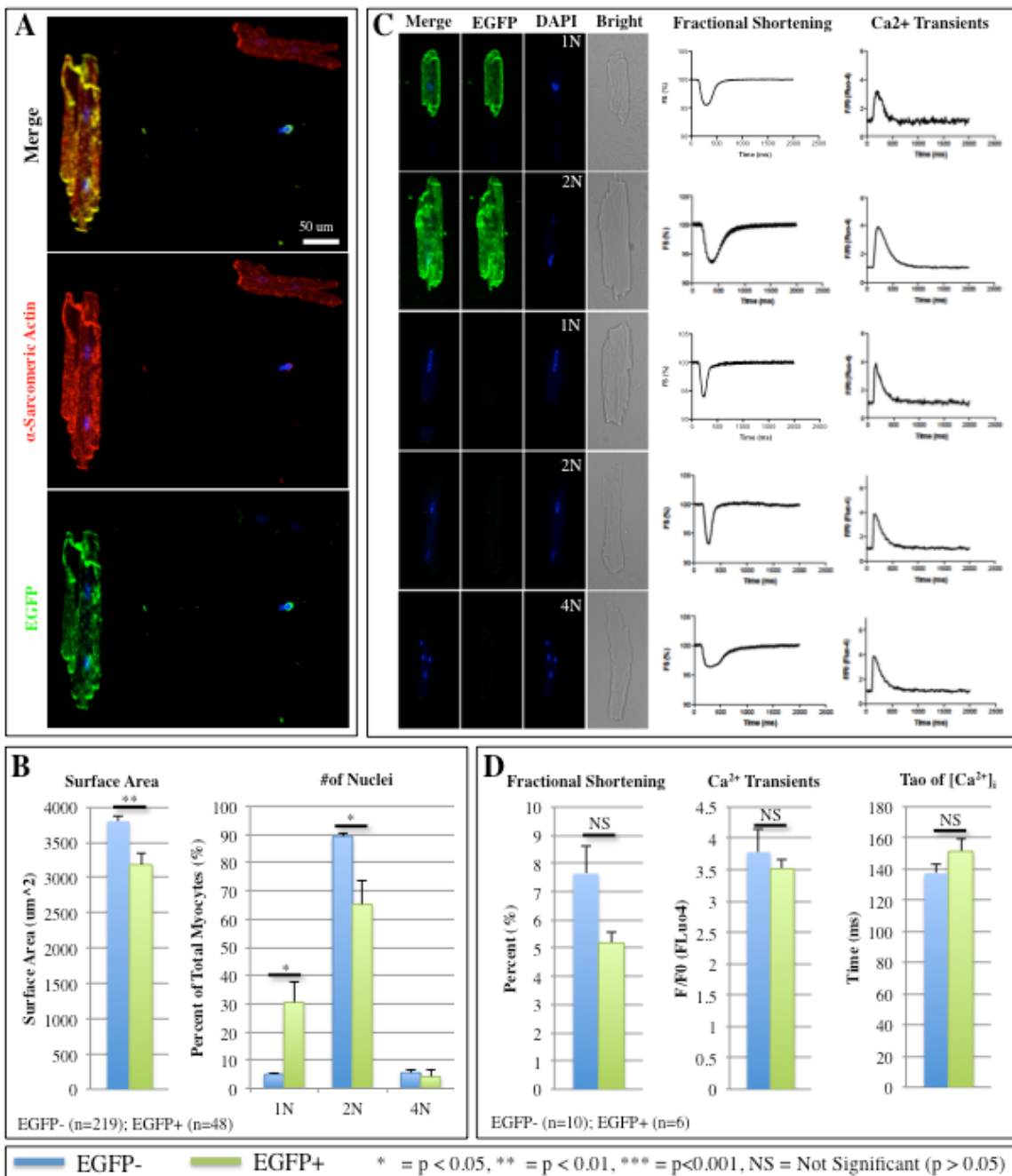


Figure 21: Cardiac stem cells grow and expand over 6 weeks but do not adopt a myocyte or vascular phenotype. Injection sites from MI animals receiving CDC treatment were sacrificed at 1, 2, or 6 weeks and were stained for A)  $\alpha$ -sarcomeric actin (red) and EGFP (green), or B) connexin43 (red), EGFP (green) and  $\alpha$ -sarcomeric actin (white). Nuclei are labeled with DAPI (blue).

EGFP+ myocytes isolated 6 weeks after injection demonstrated mature contractile properties

Some animals that received MI and CBSC therapy were sacrificed 6 weeks after injury and myocytes from their left ventricles were isolated and studied *in vitro*. Isolated myocytes were also immunostained against α-sarcomeric actin (red), EGFP (green) and nuclei were labeled with DAPI (blue) in order analyze myocyte size and the number of nuclei per cell (Figure 22). Of all the myocytes in the left ventricle, an estimated 0.84% expressed EGFP, suggesting that these cells had been derived from transplanted CBSCs. In order to estimate how many new myocytes were formed from EGFP+ CBSCs (assuming that 0.84% of isolated myocytes were EGFP+), the total number and volume of myocytes in the heart must be calculated. Our lab has previously estimated the total number of ventricular myocytes in the feline heart<sup>80</sup> by measuring the average volume of the animal heart and the average volume of a myocyte. The mean weights of the mouse heart 6 weeks post-MI+CBSC =  $205.3 \pm 10.8$  mg and the average volume of a mouse myocyte can be estimated using average myocyte dimensions ( $100 \times 20 \times 10 \text{ } \mu\text{m} = 20,000 \text{ } \mu\text{m}^3 = 2 \times 10^{-8}$  mL). If the density of myocardial tissues =  $1.06 \text{ mg/mm}^3$ ,<sup>81</sup> than the average volume of hearts at 6 weeks post-MI+CBSC =  $205.3 / 1.06 = 195.5 \text{ mm}^3 = 0.1955 \text{ mL}$ . Myocytes are known to make up 80% of the heart by volume,<sup>82</sup> so the volume of the heart constituting myocytes =  $0.8 \times 0.1955 = 0.1564 \text{ mL}$ . Thus, the total number of new EGFP+ myocytes in the average mouse heart at 6 weeks post-MI+CBSC =  $0.1564 \text{ mL} / 2 \times 10^{-8} \text{ mL} = 7.8 \times 10^6$  total



**Figure 22: Isolated myocyte size, number of nuclei, and cell physiology were analyzed 6 weeks post-MI.** **A)** Myocytes were immunostained against  $\alpha$ -sarcomeric actin (red), EGFP (green), and DAPI (blue). **B)** Average surface area of EGFP+ versus EGFP- myocytes and percent of total EGFP+ or EGFP- cells

that were mono-, bi-, or tetranucleated. **C)** Representative fractional shortening and  $\text{Ca}^{2+}$  transients of EGFP+ myocytes with 1 or 2 nuclei, or EGFP- myocytes with 1, 2, or 4 nuclei. **D)** Mean fractional shortening, peak  $\text{Ca}^{2+}$  F/F<sub>0</sub>, and the time constant of decay (t) of  $\text{Ca}^{2+}$  transients for all EGFP+ versus EGFP- myocytes.

myocytes/heart. According to our analysis, if 0.84% of myocytes analyzed were positive for EGFP, than  $0.0084 \times 7.8 \times 10^6 = 65,688$  new EGFP+ myocytes were formed per heart. At the time of surgery, 40,000 cells were initially injected, so the cells must have proliferated by at least 150% after injection into the heart.

EGFP+ myocytes were identified, and the size and number of nuclei per cell were analyzed and compared to EGFP- myocytes isolated from the same hearts. Figure 22A shows a representative EGFP+ myocyte with two nuclei. When compared to EGFP- controls, EGFP+ myocytes had smaller average cross-sectional surface area (Figure 22B). Over 90% of EGFP- myocytes were binucleated, while only 5.4% of EGFP- cells were mononucleated and 4.1% were tetranucleated. In contrast, there were significantly more mononucleated and significantly fewer binucleated EGFP+ myocytes, with 1/3 EGFP+ myocytes having only one nucleus (Figure 22B). There was no significant difference in tetranucleation between EGFP+ and EGFP- myocytes.

Isolated EGFP+ and EGFP- myocyte fractional shortening (FS) and  $\text{Ca}^{2+}$  currents were then analyzed *in vitro*. Figure 22C shows representative EGFP+ and EGFP- myocytes under fluorescence or bright field histology with their corresponding FS or  $\text{Ca}^{2+}$  transients. Mean FS, peak  $\text{Ca}^{2+}$  ( $F/F_0$ ) and time constant of decay of the  $\text{Ca}^{2+}$  transients are shown in Figure 22D. EGFP+ myocytes isolated 6 weeks after MI had contractions and  $\text{Ca}^{2+}$  transients that were indistinguishable from EGFP- controls.

## CHAPTER 8: DISCUSSION

This study explored the potential beneficial effects of transplanting a novel population of c-kit+/Sca-1+ cells (from the stem cell niches within the bone, rather than from bone marrow) into the border zone of a myocardial infarction, and the effects of this novel cell type was compared to a widely-studied population of c-kit+/Sca-1+ cardiac-derived stem cells. Our results show that CBSCs have beneficial effects on the structure and function of the heart after MI. Animals with MI that received a CBSC transplant had improved 6-week survival, cardiac function, and attenuation of adverse left ventricular remodeling compared with both saline-injected MI controls and CDC-treated MI animals. Strain analysis demonstrated that CBSC-treated MI animals not only had improved global function, but their hearts also had greater contractile activity at the MI border zone relative to saline- and CDC-injected hearts. Strain analysis allows for precise imaging at the infarct border zone where stem cells were specifically administered to achieve maximal effect,<sup>69</sup> and where new myocardium was detected using histological techniques. Strain analysis of these CBSC-treated border zone segments clearly show enhanced contraction (Figure 9A-B), suggesting that the stem cells regenerated contractile tissues. Histological analysis showed that, while CDCs failed to adopt adult phenotypes, EGFP+ stem cell-derived adult cardiac myocytes with normally striated  $\alpha$ -sarcomeric actin networks and connexin43+ gap junctions were present throughout the border zone in CBSC treated mice (Figure 15C), in areas that had robust contractile

function on strain analysis, supporting the idea that newly formed cardiac muscle was derived from injected CBSCs. CBSC-derived new cardiac myocytes that were isolated from hearts 6 weeks after MI had normal contractions and Ca<sup>2+</sup> transients.

**CBSCs secrete pro-angiogenic factors and promote neovascularization**

A major goal of the present study was to explore paracrine effects of injected CBSCs. Many studies have looked at stem cell paracrine factors *in vitro*, but to our knowledge, ours is the first study to comprehensively examine how the expression of these factors changes after transplant.<sup>54, 73-78, 83</sup> We specifically explored neovascularization in regions with injected CBSCs. Our studies showed that CBSCs produced the pro-angiogenic factors bFGF and VEGF (both *in vitro* and *in vivo*). These factors are known to be involved in vascular cell proliferation and induction of angiogenesis,<sup>48, 72-75, 77, 78</sup> and there was evidence of increased neovascularization in the infarct zone of hearts treated with stem cells in this study (Figure 13). Although CDCs initially produced Ang-1 in addition to bFGF and VEGF, the expression of these factors was not sustained past 24 hours post-MI and the neovascularization of the border zone in CDC treated animals was less robust than CBSC-treated animals by 6 weeks post-MI. Additionally, our studies showed that, while CDCs did not transdifferentiate by 6 weeks post-MI, CBSCs transdifferentiated into adult vascular cells, including smooth muscle and endothelial cells, although this was observed relatively infrequently. While there was robust evidence of myocyte transdifferentiation

(EGFP+ cardiac myocytes were identified in 5/8 hearts analyzed 6 weeks post-MI), and many cells from hearts at earlier time points could be identified in intermediate stages of differentiation down the myocyte lineage (in 6/6 hearts fixed after 1 week post-MI+CBSC and in 3/3 hearts fixed at 2 weeks Post-MI+CBSC), the same could not be said for cells of the vascular lineage (EGFP+ vascular cells were only identified in 2/8 hearts analyzed at 6 weeks post-MI and no intermediate EGFP+ lumen or tube like structures were found at 1 or 2 weeks post-MI). These findings suggest that paracrine-induced new blood vessel formation appears to be the primary mechanism for the enhanced angiogenesis observed in CBSC-injected hearts. The *in vivo* paracrine factor analysis showed those factors involved in cardioprotection (HGF, IGF) or stimulation of endogenous stem cells (SCF, SDF1) that were expressed in CBSCs *in vitro* were not found in CBSCs after they were injected into the MI border zone. These results suggest that part of the beneficial effect of CBSCs on MI hearts is paracrine-mediated enhancement of angiogenesis.

#### CBSCs differentiate into new cardiac myocytes

In the present study we used CBSCs and CDCs from an EGFP+ mouse so that we could easily trace the fate of the injected cells. Using time course *in vivo* histological analysis with this stably expressed fluorophore, we were able to demonstrate that CBSCs differentiated over time down the myocyte lineage by 6 weeks post-MI while CDCs did not. Previous studies that did not observe transdifferentiation may have missed these observations because they have

analyzed only a single follow-up time point<sup>4</sup> or have used timepoints that would have been much too early to observe differentiation.<sup>56</sup> Other studies have utilized conditionally expressed labels (i.e. β-galactosidase expressed off of the alpha-MHC promotor, which is only activated after differentiation), and may have missed some of the intermediate stages of differentiation that our study was able to detect.<sup>84</sup> As discussed above, we found evidence for enhanced revascularization of the MI border and infarct zone in CBSC injected hearts. However, the new blood vessels were rarely comprised of EGFP+ cells, suggesting that CBSCs enhanced endogenous repair. Our experiments demonstrate that EGFP+ CBSCs express cardiac proteins soon after injection into the MI heart, and by 6 weeks post-MI these cells have organized sarcomeres, are connected to their neighbors via gap junctions, and contract with Ca<sup>2+</sup> transients that are similar to those of EGFP- myocytes isolated from the same hearts. None of these observations were seen in CDC-treated animals.

Our studies suggest that the transition from an injected CBSC to a fully functional cardiac myocyte takes between 2-6 weeks. After one week most the EGFP+ cells had immature characteristics and expressed unorganized cardiac contractile proteins. Two weeks after MI areas with EGFP+ cells were larger, suggesting cell proliferation, and the cells had begun to elongate along the axis of EGFP- myocytes that had survived the infarct. More EGFP+ cells expressed cardiac contractile proteins but no organized sarcomeres were found. By 6 weeks post-MI there were many regions containing EGFP+ myocytes with organized sarcomeres and these cells were well integrated in the myocardium

via gap junctions. The contribution of these new myocytes to the improved cardiac contractile performance of the post-MI heart cannot be proven with the techniques used in these experiments. However, regional strain measurements from sites of CBSC injection documented increased contractile performance in the regions where we isolated EGFP+ myocytes with robust contractile activity. These findings support the idea that CBSC-mediated new myocyte formation is at least partially responsible for improvements in cardiac structure and function in MI hearts with CBSC treatments.

Our major evidence for CBSC-derived new myocyte formation is that we found EGFP+ cardiac myocytes in the MI border zone of hearts 6 weeks after CBSC injections. There is always concern that injected cells might have fused with existing myocytes,<sup>85</sup> but little or no evidence for fusion in these types of experiments has been observed.<sup>3, 86</sup> We also have evidence that the EGFP+ myocytes we found were newly formed from smaller CBSC progeny. Our experiments showed that EGFP+ isolated myocytes were smaller and a higher percentage of these cells were mononucleated, consistent with a maturing adult cardiac myocyte. These data are consistent with previously published reports from our laboratory in which newly formed myocytes were detected in the growing heart during adolescence.<sup>80</sup> Collectively our results suggest that CBSCs survive in the MI border zone and within weeks they begin to form new cardiac tissue. The survival and differentiation of CBSCs was associated with improved cardiac structure and function and enhanced survival.

### Other CBSC cardioprotective effects

Our experiments show improved cardiac structure and function in the first two weeks after MI, before injected cells had enhanced vascularity and local contractility. The mechanisms of these early beneficial effects are not clear. One possibility is that injected cells thicken and stabilize the infarcted wall, thereby reducing wall stress and slowing dilation. These results are consistent with early stage clinical trials with wall stabilizing agents.<sup>87, 88</sup> The cardiac functional data of MI animals treated with CDCs and CBSCs also provide some insight into the wall stabilizing effect of cell therapy. By 1 week post-MI, both the MI+CDC and MI+CBSC groups had similar cardiac functional parameters (ejection fraction and fractional shortening). However, with time the functional improvements in the MI+CBSC group were sustained while the function in MI+CDC animals continued to decline. The initial functional benefit may be attributed to a wall stabilizing effect that would likely be the same between both cell types, while the sustained functional improvement seen only in the MI+CBSC group could be the result of transdifferentiation and contribution of contractile forces by newly formed myocytes.

### CBSCs versus CDCs and other stem cell types

Overall our data suggests that a bone derived c-kit+/Sca-1+ stem cell population can support the injured heart through direct transdifferentiation into adult cardiomyocytes and vascular cells as well as through secretion of proangiogenic paracrine factors. In all parameters throughout this study, CBSCs

proved more adept at supporting the injured heart than CDCs, and only CBSCs showed the capacity to transdifferentiate and form cells with adult phenotypes in this animal model. We believe that cortical bone provides an easy-to-access, more abundant source of stem cells that are potentially more pluripotent than has previously been isolated from the bone marrow or the heart. Additionally, these stem cells can be isolated from cortical bone in high numbers without the need for arduous sorting processes such as FACS or magnetic bead sorting that are required to isolate the relatively rare populations of c-kit+ cells from the bone marrow or myocardium.

Previously, there has been much skepticism that cells from outside the heart are capable of cardiomyogenesis,<sup>84, 89</sup> and many researchers have argued that new myocytes in stem cell treated hearts are derived from paracrine stimulation of endogenous stem cells.<sup>48, 56</sup> Our study shows that bone-derived stem cells can directly form new myocytes, independently of endogenous CDCs, and these new myocytes can be isolated and their contractile properties are indistinguishable from endogenous myocytes. Transplanted CDCs in our model failed to produce any cells with mature adult phenotypes, suggesting that they lack the potential or have an impaired capacity to transdifferentiate within 6 weeks after MI. Additionally, our stem cells have shown a wide potential to support the injured heart through several mechanisms without modification, while other groups have relied on viruses or plasmids to modify less effective stem cells to make them function better.<sup>74, 75, 90, 91</sup> Perhaps the key to unlocking the

success of future stem cell therapies is not through manipulation, but rather through finding the best type stem cell for the clinical application.

In summary, our studies show that CBSCs can survive the hostile environment of the post-MI heart without modification, secrete factors that enhance endogenous angiogenesis-mediated repair, and differentiate into new cardiac tissue. These beneficial effects culminate in a heart with less structural remodeling and improved cardiac pump function.

## CHAPTER 9: FUTURE DIRECTIONS FOR CARDIAC CELL THERAPY

Stem cell-based therapies have shown safety and promise in clinical trials, but further improvements are clearly needed to expand upon the moderate functional improvements that stem cells have been shown to offer in both preclinical and clinical trials. In this study, we have identified a novel population of bone-derived stem cells that may be better suited at inducing cardiac repair than previously studied cardiac or bone marrow-derived stem cells. In addition to optimizing the type of stem cells used for these studies, several new strategies have been proposed that, at least in preclinical studies, may hold promise as potential adjuncts to stem cell-based therapies. The use of biomaterials may improve cardiac function increase cell engraftment, while the use of decellularized myocardium or extracellular matrix-derived scaffolds may direct stem cell differentiation and tissue regeneration. Finally, genes have recently been discovered that, when delivered into any somatic cell can reprogram that cell into a stem-like phenotype and induce cardiac regeneration.

### Biomaterials

As stated in Chapter 1, a major problem with current cell-based regeneration strategies is the low rate of engraftment and long-term retention of stem cells by the ischemic myocardium. Implantation of stem cells embedded in a biomaterial or matrix that can improve their engraftment and hold them within damaged tissues may be key to enhancing future therapies. Many types of

materials have been tested in animal studies. One such material is Matrigel, which is a basement membrane-rich protein mixture that is isolated from Engelbreth-Holm-Swarm mouse sarcoma tumors and has been shown to induce stem cell differentiation.<sup>92</sup> When Matrigel was mixed with mouse embryonic stem cells and injected into a mouse model of MI, cardiac function was significantly improved relative to mice treated only with Matrigel or only with embryonic stem cells.<sup>93</sup> Another factor that makes Matrigel particularly well suited for use with stem cells to treat heart disease is that it is a liquid when cooled but it hardens into a solid gel at body temperature, a property that would allow it to easily be injected through a catheter for interventional cardiac stem cell therapies.

Another material with great potential as an adjuvant for stem cell therapy is alginate, a biopolymer derived from brown seaweed. This material, like Matrigel, has elastic properties that have been shown to stabilize the infarcted wall when injected alone into a rat MI model and can improve cardiac function.<sup>87</sup> Also like Matrigel, alginate is a liquid with lower viscosity at room temperature and it hardens into a gel at body temperature, making it particularly well suited for catheter-based delivery. However, the functional benefits associated with alginate polymer injection alone are merely mechanical and non-regenerative, and their administration in combination with cardiogenic stem cells remains to be tested. However, both substrates may enhance the degree of stem cell engraftment and could dramatically improve the outcome of regenerative therapies when added to the mix with cardiogenic stem cells.

### Decellularization and Extracellular Matrix-derived Scaffolds

Another matrix with vast potential to enhance current stem cells therapies is the extracellular matrix (ECM). ECM proteins have long been hypothesized to direct progenitor cell differentiation and encourage stem cell development into a particular tissue. A 2008 study first demonstrated the capacity for whole hearts to be decellularized by perfusion digestion with 1% SDS, re-perfused with cardiogenic stem cells, incubated in a sterile bioreactor and regrown into viable donor hearts.<sup>94</sup> The authors in this study demonstrated that SDS perfusion completely eliminated host immune cells and MHC complexes from the donor scaffold, so ECM-based tissues could potentially be generated using autologous stem cells and transplanted into a recipient without risk of inducing an allogeneic immune response. Donor organs like hearts are exceedingly rare across the US and throughout the world, and this type of *ex vivo* organogenesis offers the potential for a wide range of new donor tissues to be used. This type of procedure would open up cadaveric and animal tissues as potential sources for ECM, since the digestion process is capable of removing MHC antigens and donor immune cells.

While generation of complex organs from ECM-based scaffolds is still in its infancy, simpler organs have been generated using similar preparations. A wide variety of procedures are being developed for generating *ex vivo* engineered skin,<sup>95</sup> and both trachea and bladders generated *ex vivo* have been successfully transplanted into human patients. A team of British and Spanish scientists were able to decellularize a cadaveric trachea and generate an

autologous graft for a 30 year old woman from Barcelona who's left main bronchus had been obliterated by tuberculosis infection. Using the recipient's own mesenchymal stem cell-derived chondrocytes, cells were isolated and expanded *ex vivo* and seeded onto the decellularized cadaveric trachea. After the transplant, the woman recovered normal respiratory function within 4 months and did not experience any immune reaction to the transplant. Using a collagen and polyglycolic acid matrix, researchers at the Wake Forrest Institute of Regenerative Medicine were able to build autologous artificial bladders by seeding the matrices with each patient's own bladder cells.<sup>96</sup> Patients receiving the artificial bladders sustained normal kidney and urinary functions as long as 5 years after transplantation.

While ECM-based regenerative procedure have so far been limited to simple tissues like the trachea or bladder, generation of complex organs may soon be possible. Especially with advances in stem cell biology, we may now be closer to finding the optimal stem cell type best suited for cardiogenesis. In combination ECM scaffolds, these cells may finally be made into complex tissues or injectable products capable of inducing cardiac regeneration on a larger scale.

### *Reprogramming and Induced-pluripotent stem cells*

The process for inducing pluripotent stem cells (iPS) from human somatic cells was first described in 2007 in dueling publications from James A. Thomson<sup>97</sup>, a researcher at the University of Wisconsin who was also the first scientist to isolate human embryonic stem cells, and Shinya Yamanaka<sup>98</sup>, a

scientist from Kyoto University in Japan who won last year's Nobel Prize in medicine for his work on iPS cells. The two research teams outlined a process by which four essential genes encoded on a large retrovirus could be infected into a human somatic cell and induce it into a multipotent embryonic stem cell-like state. Dr. Thomson's research team used the four factors Oct4, Sox2, Nanog, and Lin28 for reprogramming, while Dr. Yamanaka's team achieved the same results using Oct4, Sox2 and c-myc and Klf4 (rather than Nanog and Lin28). While the two protocols differ slightly, both studies demonstrated the promise of iPS cell technology, which could offer vast sources of multipotent embryonic-like cells that can be generated without all of the ethical controversy surrounding embryonic stem cells.

Since these initial groundbreaking discoveries, scientists have been investigating whether it was possible to reprogram adult cells into more committed adult progenitors capable of regenerating specific tissue types. In the heart, Eric Olsen<sup>14</sup> at University of Texas-Southwest and Deepak Srivastava<sup>13</sup> at University of California-San Francisco have both developed similar strategies for converting cardiac fibroblasts into cardiomyocytes. Fibroblasts, the major parenchymal cell of the heart, account for the majority of the cells in the heart by number,<sup>13, 14</sup> and up to 95% of non-myocytes in the heart.<sup>99</sup> Thus the cardiac fibroblast population represents a large cellular pool that could be induced to form new cardiomyocytes following a large cardiac tissue injury such as MI. Both groups agree that three genes encoding cardiac transcription factors are required for induced cardiomyogenesis: Gata-4, Mef2c, and Tbx5. Additionally, the Olsen

lab argues that a fourth gene, Hand-2, further enhances cardiomyogenesis. Using mouse models of MI published in Nature last year, both groups demonstrated that their cocktail of genes could potently induce cardiac repair. Each group used fate-mapping approaches to prove that new cardiomyocytes were formed specifically from cardiac fibroblasts.<sup>13, 14</sup>

### Conclusions

In this report, 24 clinical trials completed in the last 15 years that used stem cells to treat heart disease were reviewed. A major issue with these trials remains finding the optimal stem cell type for achieving cardiac repair. In this study on bone-derived stem cells, we have offered concrete evidence that CBSCs can improve cardiac function after transplant through paracrine signaling mechanisms that recruit new blood vessels and through direct transdifferentiation into adult cardiomyocytes that can contribute functional contractile forces to the injured heart. CBSCs are easier to isolate than a more widely studied population of cardiac-derived stem cells, and we have also offered evidence that CBSCs offer greater functional improvements than CDCs (which do not appear to fully differentiate into adult cells in our animal model). Finally, several future directions have been offered for how to continue improving cell therapies in the future, including use of biomaterials or extracellular matrices as well as through use of viral vectors to induce pluripotent stem cells to form within the damaged heart.

## REFERENCES

1. Pfeffer MA, Braunwald E. Ventricular remodeling after myocardial infarction. Experimental observations and clinical implications. *Circulation*. 1990;81:1161-1172
2. Gomez AM, Guatimosim S, Dilly KW, Vassort G, Lederer WJ. Heart failure after myocardial infarction: Altered excitation-contraction coupling. *Circulation*. 2001;104:688-693
3. Beltrami AP, Barlucchi L, Torella D, Baker M, Limana F, Chimenti S, Kasahara H, Rota M, Musso E, Urbanek K, Leri A, Kajstura J, Nadal-Ginard B, Anversa P. Adult cardiac stem cells are multipotent and support myocardial regeneration. *Cell*. 2003;114:763-776
4. Tang XL, Rokosh G, Sanganalmath SK, Yuan F, Sato H, Mu J, Dai S, Li C, Chen N, Peng Y, Dawn B, Hunt G, Leri A, Kajstura J, Tiwari S, Shirk G, Anversa P, Bolli R. Intracoronary administration of cardiac progenitor cells alleviates left ventricular dysfunction in rats with a 30-day-old infarction. *Circulation*. 2010;121:293-305
5. Rota M, Padin-Iruegas ME, Misao Y, De Angelis A, Maestroni S, Ferreira-Martins J, Fiumana E, Rastaldo R, Arcarese ML, Mitchell TS, Boni A, Bolli R, Urbanek K, Hosoda T, Anversa P, Leri A, Kajstura J. Local activation or implantation of cardiac progenitor cells rescues scarred infarcted myocardium improving cardiac function. *Circ Res*. 2008;103:107-116
6. Smith RR, Barile L, Cho HC, Leppo MK, Hare JM, Messina E, Giacomello A, Abraham MR, Marban E. Regenerative potential of cardiosphere-derived cells expanded from percutaneous endomyocardial biopsy specimens. *Circulation*. 2007;115:896-908
7. Orlic D, Kajstura J, Chimenti S, Jakoniuk I, Anderson SM, Li B, Pickel J, McKay R, Nadal-Ginard B, Bodine DM, Leri A, Anversa P. Bone marrow cells regenerate infarcted myocardium. *Nature*. 2001;410:701-705
8. Rota M, Kajstura J, Hosoda T, Bearzi C, Vitale S, Esposito G, Iaffaldano G, Padin-Iruegas ME, Gonzalez A, Rizzi R, Small N, Muraski J, Alvarez R, Chen X, Urbanek K, Bolli R, Houser SR, Leri A, Sussman MA, Anversa P. Bone marrow cells adopt the cardiomyogenic fate in vivo. *Proc Natl Acad Sci U S A*. 2007;104:17783-17788
9. Mauritz C, Schwanke K, Reppel M, Neef S, Katsirntaki K, Maier LS, Nguemo F, Menke S, Haustein M, Hescheler J, Hasenfuss G, Martin U.

- Generation of functional murine cardiac myocytes from induced pluripotent stem cells. *Circulation*. 2008;118:507-517
10. Zhang J, Wilson GF, Soerens AG, Koonce CH, Yu J, Palecek SP, Thomson JA, Kamp TJ. Functional cardiomyocytes derived from human induced pluripotent stem cells. *Circ Res*. 2009;104:e30-41
  11. Zwi L, Caspi O, Arbel G, Huber I, Gepstein A, Park IH, Gepstein L. Cardiomyocyte differentiation of human induced pluripotent stem cells. *Circulation*. 2009;120:1513-1523
  12. Nelson TJ, Ge ZD, Van Orman J, Barron M, Rudy-Reil D, Hacker TA, Misra R, Duncan SA, Auchampach JA, Lough JW. Improved cardiac function in infarcted mice after treatment with pluripotent embryonic stem cells. *Anat Rec A Discov Mol Cell Evol Biol*. 2006;288:1216-1224
  13. Qian L, Huang Y, Spencer CI, Foley A, Vedantham V, Liu L, Conway SJ, Fu JD, Srivastava D. In vivo reprogramming of murine cardiac fibroblasts into induced cardiomyocytes. *Nature*. 2012;485:593-598
  14. Song K, Nam YJ, Luo X, Qi X, Tan W, Huang GN, Acharya A, Smith CL, Tallquist MD, Neilson EG, Hill JA, Bassel-Duby R, Olson EN. Heart repair by reprogramming non-myocytes with cardiac transcription factors. *Nature*. 2012;485:599-604
  15. Strauer BE, Brehm M, Zeus T, Kostering M, Hernandez A, Sorg RV, Kogler G, Wernet P. Repair of infarcted myocardium by autologous intracoronary mononuclear bone marrow cell transplantation in humans. *Circulation*. 2002;106:1913-1918
  16. Assmus B, Schachinger V, Teupe C, Britten M, Lehmann R, Dobert N, Grunwald F, Aicher A, Urbich C, Martin H, Hoelzer D, Dimmeler S, Zeiher AM. Transplantation of progenitor cells and regeneration enhancement in acute myocardial infarction (topcare-ami). *Circulation*. 2002;106:3009-3017
  17. Britten MB, Abolmaali ND, Assmus B, Lehmann R, Honold J, Schmitt J, Vogl TJ, Martin H, Schachinger V, Dimmeler S, Zeiher AM. Infarct remodeling after intracoronary progenitor cell treatment in patients with acute myocardial infarction (topcare-ami): Mechanistic insights from serial contrast-enhanced magnetic resonance imaging. *Circulation*. 2003;108:2212-2218
  18. Schachinger V, Assmus B, Britten MB, Honold J, Lehmann R, Teupe C, Abolmaali ND, Vogl TJ, Hofmann WK, Martin H, Dimmeler S, Zeiher AM. Transplantation of progenitor cells and regeneration enhancement in

- acute myocardial infarction: Final one-year results of the topcare-ami trial. *J Am Coll Cardiol.* 2004;44:1690-1699
19. Stamm C, Westphal B, Kleine HD, Petzsch M, Kittner C, Klinge H, Schumichen C, Nienaber CA, Freund M, Steinhoff G. Autologous bone-marrow stem-cell transplantation for myocardial regeneration. *Lancet.* 2003;361:45-46
  20. Perin EC, Dohmann HF, Borojevic R, Silva SA, Sousa AL, Mesquita CT, Rossi MI, Carvalho AC, Dutra HS, Dohmann HJ, Silva GV, Belem L, Vivacqua R, Rangel FO, Esporcatte R, Geng YJ, Vaughn WK, Assad JA, Mesquita ET, Willerson JT. Transendocardial, autologous bone marrow cell transplantation for severe, chronic ischemic heart failure. *Circulation.* 2003;107:2294-2302
  21. Kuethe F, Richartz BM, Sayer HG, Kasper C, Werner GS, Hoffken K, Figulla HR. Lack of regeneration of myocardium by autologous intracoronary mononuclear bone marrow cell transplantation in humans with large anterior myocardial infarctions. *Int J Cardiol.* 2004;97:123-127
  22. Chen SL, Fang WW, Ye F, Liu YH, Qian J, Shan SJ, Zhang JJ, Chunhua RZ, Liao LM, Lin S, Sun JP. Effect on left ventricular function of intracoronary transplantation of autologous bone marrow mesenchymal stem cell in patients with acute myocardial infarction. *Am J Cardiol.* 2004;94:92-95
  23. Wollert KC, Meyer GP, Lotz J, Ringes-Lichtenberg S, Lippolt P, Breidenbach C, Fichtner S, Korte T, Hornig B, Messinger D, Arseniev L, Hertenstein B, Ganser A, Drexler H. Intracoronary autologous bone-marrow cell transfer after myocardial infarction: The boost randomised controlled clinical trial. *Lancet.* 2004;364:141-148
  24. Meyer GP, Wollert KC, Lotz J, Pirr J, Rager U, Lippolt P, Hahn A, Fichtner S, Schaefer A, Arseniev L, Ganser A, Drexler H. Intracoronary bone marrow cell transfer after myocardial infarction: 5-year follow-up from the randomized-controlled boost trial. *Eur Heart J.* 2009;30:2978-2984
  25. Bartunek J, Vanderheyden M, Vandekerckhove B, Mansour S, De Bruyne B, De Bondt P, Van Haute I, Lootens N, Heyndrickx G, Wijns W. Intracoronary injection of cd133-positive enriched bone marrow progenitor cells promotes cardiac recovery after recent myocardial infarction: Feasibility and safety. *Circulation.* 2005;112:I178-183
  26. Strauer BE, Brehm M, Zeus T, Bartsch T, Schannwell C, Antke C, Sorg RV, Kogler G, Wernet P, Muller HW, Kostering M. Regeneration of human infarcted heart muscle by intracoronary autologous bone marrow cell

- transplantation in chronic coronary artery disease: The iact study. *J Am Coll Cardiol.* 2005;46:1651-1658
27. Janssens S, Dubois C, Bogaert J, Theunissen K, Deroose C, Desmet W, Kalantzi M, Herbots L, Sinnaeve P, Dens J, Maertens J, Rademakers F, Dymarkowski S, Gheysens O, Van Cleemput J, Bormans G, Nuyts J, Belmans A, Mortelmans L, Boogaerts M, Van de Werf F. Autologous bone marrow-derived stem-cell transfer in patients with st-segment elevation myocardial infarction: Double-blind, randomised controlled trial. *Lancet.* 2006;367:113-121
  28. Ge J, Li Y, Qian J, Shi J, Wang Q, Niu Y, Fan B, Liu X, Zhang S, Sun A, Zou Y. Efficacy of emergent transcatheter transplantation of stem cells for treatment of acute myocardial infarction (tct-stami). *Heart.* 2006;92:1764-1767
  29. Lunde K, Solheim S, Aakhus S, Arnesen H, Abdelnoor M, Egeland T, Endresen K, Illebekk A, Mangschau A, Fjeld JG, Smith HJ, Taraldsrud E, Groggaard HK, Bjornerheim R, Brekke M, Muller C, Hopp E, Ragnarsson A, Brinchmann JE, Forfang K. Intracoronary injection of mononuclear bone marrow cells in acute myocardial infarction. *N Engl J Med.* 2006;355:1199-1209
  30. Schachinger V, Erbs S, Elsasser A, Haberbosch W, Hambrecht R, Holschermann H, Yu J, Corti R, Mathey DG, Hamm CW, Suselbeck T, Assmus B, Tonn T, Dimmeler S, Zeiher AM. Intracoronary bone marrow-derived progenitor cells in acute myocardial infarction. *N Engl J Med.* 2006;355:1210-1221
  31. Schachinger V, Erbs S, Elsasser A, Haberbosch W, Hambrecht R, Holschermann H, Yu J, Corti R, Mathey DG, Hamm CW, Suselbeck T, Werner N, Haase J, Neuzner J, Germing A, Mark B, Assmus B, Tonn T, Dimmeler S, Zeiher AM. Improved clinical outcome after intracoronary administration of bone-marrow-derived progenitor cells in acute myocardial infarction: Final 1-year results of the repair-ami trial. *Eur Heart J.* 2006;27:2775-2783
  32. Assmus B, Rolf A, Erbs S, Elsasser A, Haberbosch W, Hambrecht R, Tillmanns H, Yu J, Corti R, Mathey DG, Hamm CW, Suselbeck T, Tonn T, Dimmeler S, Dill T, Zeiher AM, Schachinger V. Clinical outcome 2 years after intracoronary administration of bone marrow-derived progenitor cells in acute myocardial infarction. *Circ Heart Fail.* 2010;3:89-96
  33. Dill T, Schachinger V, Rolf A, Mollmann S, Thiele H, Tillmanns H, Assmus B, Dimmeler S, Zeiher AM, Hamm C. Intracoronary administration of bone marrow-derived progenitor cells improves left ventricular function in

- patients at risk for adverse remodeling after acute st-segment elevation myocardial infarction: Results of the reinfusion of enriched progenitor cells and infarct remodeling in acute myocardial infarction study (repair-ami) cardiac magnetic resonance imaging substudy. *Am Heart J.* 2009;157:541-547
34. Meluzin J, Mayer J, Groch L, Janousek S, Hornacek I, Hlinomaz O, Kala P, Panovsky R, Prasek J, Kaminek M, Stanicek J, Klabusay M, Koristek Z, Navratil M, Dusek L, Vinklarkova J. Autologous transplantation of mononuclear bone marrow cells in patients with acute myocardial infarction: The effect of the dose of transplanted cells on myocardial function. *Am Heart J.* 2006;152:975 e979-915
  35. Penicka M, Horak J, Kobylka P, Pytlík R, Kozak T, Belohlavek O, Lang O, Skalicka H, Simek S, Palecek T, Linhart A, Aschermann M, Widimsky P. Intracoronary injection of autologous bone marrow-derived mononuclear cells in patients with large anterior acute myocardial infarction: A prematurely terminated randomized study. *J Am Coll Cardiol.* 2007;49:2373-2374
  36. Tatsumi T, Ashihara E, Yasui T, Matsunaga S, Kido A, Sasada Y, Nishikawa S, Hadase M, Koide M, Nakamura R, Irie H, Ito K, Matsui A, Matsui H, Katamura M, Kusuoka S, Matoba S, Okayama S, Horii M, Uemura S, Shimazaki C, Tsuji H, Saito Y, Matsubara H. Intracoronary transplantation of non-expanded peripheral blood-derived mononuclear cells promotes improvement of cardiac function in patients with acute myocardial infarction. *Circ J.* 2007;71:1199-1207
  37. Cao F, Sun D, Li C, Narsinh K, Zhao L, Li X, Feng X, Zhang J, Duan Y, Wang J, Liu D, Wang H. Long-term myocardial functional improvement after autologous bone marrow mononuclear cells transplantation in patients with st-segment elevation myocardial infarction: 4 years follow-up. *Eur Heart J.* 2009;30:1986-1994
  38. Yousef M, Schannwell CM, Kostering M, Zeus T, Brehm M, Strauer BE. The balance study: Clinical benefit and long-term outcome after intracoronary autologous bone marrow cell transplantation in patients with acute myocardial infarction. *J Am Coll Cardiol.* 2009;53:2262-2269
  39. Yao K, Huang R, Sun A, Qian J, Liu X, Ge L, Zhang Y, Zhang S, Niu Y, Wang Q, Zou Y, Ge J. Repeated autologous bone marrow mononuclear cell therapy in patients with large myocardial infarction. *Eur J Heart Fail.* 2009;11:691-698
  40. Williams AR, Trachtenberg B, Velazquez DL, McNiece I, Altman P, Rouy D, Mendizabal AM, Pattany PM, Lopera GA, Fishman J, Zambrano JP,

- Heldman AW, Hare JM. Intramyocardial stem cell injection in patients with ischemic cardiomyopathy: Functional recovery and reverse remodeling. *Circ Res*. 2011;108:792-796
41. Trachtenberg B, Velazquez DL, Williams AR, McNiece I, Fishman J, Nguyen K, Rouy D, Altman P, Schwarz R, Mendizabal A, Oskouei B, Byrnes J, Soto V, Tracy M, Zambrano JP, Heldman AW, Hare JM. Rationale and design of the transendocardial injection of autologous human cells (bone marrow or mesenchymal) in chronic ischemic left ventricular dysfunction and heart failure secondary to myocardial infarction (tac-hft) trial: A randomized, double-blind, placebo-controlled study of safety and efficacy. *Am Heart J*. 2011;161:487-493
  42. Bolli R, Chugh AR, D'Amario D, Loughran JH, Stoddard MF, Ikram S, Beache GM, Wagner SG, Leri A, Hosoda T, Sanada F, Elmore JB, Goichberg P, Cappetta D, Solankhi NK, Fahsah I, Rokosh DG, Slaughter MS, Kajstura J, Anversa P. Cardiac stem cells in patients with ischaemic cardiomyopathy (scipio): Initial results of a randomised phase 1 trial. *Lancet*. 2011;378:1847-1857
  43. Makkar RR, Smith RR, Cheng K, Malliaras K, Thomson LE, Berman D, Czer LS, Marban L, Mendizabal A, Johnston PV, Russell SD, Schuleri KH, Lardo AC, Gerstenblith G, Marban E. Intracoronary cardiosphere-derived cells for heart regeneration after myocardial infarction (caduceus): A prospective, randomised phase 1 trial. *Lancet*. 2012;379:895-904
  44. Perin EC, Willerson JT, Pepine CJ, Henry TD, Ellis SG, Zhao DX, Silva GV, Lai D, Thomas JD, Kronenberg MW, Martin AD, Anderson RD, Traverse JH, Penn MS, Anwaruddin S, Hatzopoulos AK, Gee AP, Taylor DA, Cogle CR, Smith D, Westbrook L, Chen J, Handberg E, Olson RE, Geither C, Bowman S, Francescon J, Baraniuk S, Piller LB, Simpson LM, Loghin C, Aguilar D, Richman S, Zierold C, Bettencourt J, Sayre SL, Vojvodic RW, Skarlatos SI, Gordon DJ, Ebert RF, Kwak M, Moye LA, Simari RD. Effect of transendocardial delivery of autologous bone marrow mononuclear cells on functional capacity, left ventricular function, and perfusion in chronic heart failure: The focus-cctrn trial. *JAMA*. 2012;307:1717-1726
  45. Traverse JH, Henry TD, Pepine CJ, Willerson JT, Zhao DX, Ellis SG, Forder JR, Anderson RD, Hatzopoulos AK, Penn MS, Perin EC, Chambers J, Baran KW, Raveendran G, Lambert C, Lerman A, Simon DI, Vaughan DE, Lai D, Gee AP, Taylor DA, Cogle CR, Thomas JD, Olson RE, Bowman S, Francescon J, Geither C, Handberg E, Kappenman C, Westbrook L, Piller LB, Simpson LM, Baraniuk S, Loghin C, Aguilar D, Richman S, Zierold C, Spoon DB, Bettencourt J, Sayre SL, Vojvodic RW, Skarlatos SI, Gordon DJ, Ebert RF, Kwak M, Moye LA, Simari RD. Effect

- of the use and timing of bone marrow mononuclear cell delivery on left ventricular function after acute myocardial infarction: The time randomized trial. *JAMA*. 2012;1-10
46. Hou D, Youssef EA, Brinton TJ, Zhang P, Rogers P, Price ET, Yeung AC, Johnstone BH, Yock PG, March KL. Radiolabeled cell distribution after intramyocardial, intracoronary, and interstitial retrograde coronary venous delivery: Implications for current clinical trials. *Circulation*. 2005;112:1150-156
  47. Nguyen PK, Lan F, Wang Y, Wu JC. Imaging: Guiding the clinical translation of cardiac stem cell therapy. *Circ Res*. 2011;109:962-979
  48. Williams AR, Hare JM. Mesenchymal stem cells: Biology, pathophysiology, translational findings, and therapeutic implications for cardiac disease. *Circ Res*. 2011;109:923-940
  49. Traverse JH, Henry TD, Pepine CJ, Willerson JT, Zhao DX, Ellis SG, Forder JR, Anderson RD, Hatzopoulos AK, Penn MS, Perin EC, Chambers J, Baran KW, Raveendran G, Lambert C, Lerman A, Simon DI, Vaughan DE, Lai D, Gee AP, Taylor DA, Cogle CR, Thomas JD, Olson RE, Bowman S, Francescon J, Geither C, Handberg E, Kappenman C, Westbrook L, Piller LB, Simpson LM, Baraniuk S, Loghin C, Aguilar D, Richman S, Zierold C, Spoon DB, Bettencourt J, Sayre SL, Vojvodic RW, Skarlatos SI, Gordon DJ, Ebert RF, Kwak M, Moye LA, Simari RD. Effect of the use and timing of bone marrow mononuclear cell delivery on left ventricular function after acute myocardial infarction: The time randomized trial. *JAMA*. 2012;308:2380-2389
  50. Civin CI, Gore SD. Antigenic analysis of hematopoiesis: A review. *J Hematother*. 1993;2:137-144
  51. Koya T, Honda S, Narita J, Watanabe H, Arakawa M, Abo T. Enrichment of c-kit+ lin- haemopoietic progenitor cells that commit themselves to extrathymic t cells in in vitro culture of appendix mononuclear cells. *Immunology*. 1999;96:447-456
  52. He JQ, Vu DM, Hunt G, Chugh A, Bhatnagar A, Bolli R. Human cardiac stem cells isolated from atrial appendages stably express c-kit. *PLoS One*. 2011;6:e27719
  53. Zeng L, Hu Q, Wang X, Mansoor A, Lee J, Feygin J, Zhang G, Suntharalingam P, Boozer S, Mhashilkar A, Panetta CJ, Swingen C, Deans R, From AH, Bache RJ, Verfaillie CM, Zhang J. Bioenergetic and functional consequences of bone marrow-derived multipotent progenitor cell transplantation in hearts with postinfarction left ventricular remodeling. *Circulation*. 2007;115:1866-1875

54. Li TS, Cheng K, Malliaras K, Smith RR, Zhang Y, Sun B, Matsushita N, Blusztajn A, Terrovitis J, Kusuoka H, Marban L, Marban E. Direct comparison of different stem cell types and subpopulations reveals superior paracrine potency and myocardial repair efficacy with cardiosphere-derived cells. *J Am Coll Cardiol.* 2012;59:942-953
55. Segers VF, Lee RT. Stem-cell therapy for cardiac disease. *Nature.* 2008;451:937-942
56. Hatzistergos KE, Quevedo H, Oskouei BN, Hu Q, Feigenbaum GS, Margitich IS, Mazhari R, Boyle AJ, Zambrano JP, Rodriguez JE, Dulce R, Pattany PM, Valdes D, Revilla C, Heldman AW, McNiece I, Hare JM. Bone marrow mesenchymal stem cells stimulate cardiac stem cell proliferation and differentiation. *Circ Res.* 2010;107:913-922
57. Anversa P, Kajstura J, Leri A, Bolli R. Life and death of cardiac stem cells: A paradigm shift in cardiac biology. *Circulation.* 2006;113:1451-1463
58. Kucia M, Dawn B, Hunt G, Guo Y, Wysoczynski M, Majka M, Ratajczak J, Rezzoug F, Ildstad ST, Bolli R, Ratajczak MZ. Cells expressing early cardiac markers reside in the bone marrow and are mobilized into the peripheral blood after myocardial infarction. *Circ Res.* 2004;95:1191-1199
59. Urbanek K, Cesselli D, Rota M, Nascimbene A, De Angelis A, Hosoda T, Bearzi C, Boni A, Bolli R, Kajstura J, Anversa P, Leri A. Stem cell niches in the adult mouse heart. *Proc Natl Acad Sci U S A.* 2006;103:9226-9231
60. Zhu H, Guo ZK, Jiang XX, Li H, Wang XY, Yao HY, Zhang Y, Mao N. A protocol for isolation and culture of mesenchymal stem cells from mouse compact bone. *Nat Protoc.* 2010;5:550-560
61. Urbanek K, Rota M, Cascapera S, Bearzi C, Nascimbene A, De Angelis A, Hosoda T, Chimenti S, Baker M, Limana F, Nurzynska D, Torella D, Rotatori F, Rastaldo R, Musso E, Quaini F, Leri A, Kajstura J, Anversa P. Cardiac stem cells possess growth factor-receptor systems that after activation regenerate the infarcted myocardium, improving ventricular function and long-term survival. *Circ Res.* 2005;97:663-673
62. Zhang H, Makarewich CA, Kubo H, Wang W, Duran JM, Li Y, Berretta RM, Koch WJ, Chen X, Gao E, Valdivia HH, Houser SR. Hyperphosphorylation of the cardiac ryanodine receptor at serine 2808 is not involved in cardiac dysfunction after myocardial infarction. *Circ Res.* 2012;110:831-840
63. Makarewich CA, Correll RN, Gao H, Zhang H, Yang B, Berretta RM, Rizzo V, Molkentin JD, Houser SR. A caveolae-targeted I-type  $Ca(2)+$  channel

- antagonist inhibits hypertrophic signaling without reducing cardiac contractility. *Circ Res.* 2012;110:669-674
64. Kubo H, Margulies KB, Piacentino V, 3rd, Gaughan JP, Houser SR. Patients with end-stage congestive heart failure treated with beta-adrenergic receptor antagonists have improved ventricular myocyte calcium regulatory protein abundance. *Circulation.* 2001;104:1012-1018
  65. Simpson P, Savion S. Differentiation of rat myocytes in single cell cultures with and without proliferating nonmyocardial cells. Cross-striations, ultrastructure, and chronotropic response to isoproterenol. *Circ Res.* 1982;50:101-116
  66. Gaughan JP, Hefner CA, Houser SR. Electrophysiological properties of neonatal rat ventricular myocytes with alpha1-adrenergic-induced hypertrophy. *Am J Physiol.* 1998;275:H577-590
  67. Kubo H, Berretta RM, Jaleel N, Angert D, Houser SR. C-kit+ bone marrow stem cells differentiate into functional cardiac myocytes. *Clin Transl Sci.* 2009;2:26-32
  68. Tarnavski O, McMullen JR, Schinke M, Nie Q, Kong S, Izumo S. Mouse cardiac surgery: Comprehensive techniques for the generation of mouse models of human diseases and their application for genomic studies. *Physiol Genomics.* 2004;16:349-360
  69. Duran JM, Taghavi S, Berretta RM, Makarewicz CA, Sharp III T, Starosta T, Udeshi F, George JC, Kubo H, Houser SR. A characterization and targeting of the infarct border zone in a swine model of myocardial infarction. *Clin Transl Sci.* 2012;5:416-421
  70. Taghavi S, Duran JM, Berretta RM, Makarewicz CA, Udeshi F, Sharp TE, Kubo H, Houser SR, George JC. Validation of transcatheter left ventricular electromechanical mapping for assessment of cardiac function and targeted transendocardial injection in a porcine ischemia-reperfusion model. *Am J Transl Res.* 2012;4:240-246
  71. Bauer M, Cheng S, Jain M, Ngoy S, Theodoropoulos C, Trujillo A, Lin FC, Liao R. Echocardiographic speckle-tracking based strain imaging for rapid cardiovascular phenotyping in mice. *Circ Res.* 2011;108:908-916
  72. Caplan AI, Dennis JE. Mesenchymal stem cells as trophic mediators. *J Cell Biochem.* 2006;98:1076-1084
  73. Gnechi M, Zhang Z, Ni A, Dzau VJ. Paracrine mechanisms in adult stem cell signaling and therapy. *Circ Res.* 2008;103:1204-1219

74. Gnechi M, He H, Liang OD, Melo LG, Morello F, Mu H, Noiseux N, Zhang L, Pratt RE, Ingwall JS, Dzau VJ. Paracrine action accounts for marked protection of ischemic heart by akt-modified mesenchymal stem cells. *Nat Med.* 2005;11:367-368
75. Gnechi M, He H, Noiseux N, Liang OD, Zhang L, Morello F, Mu H, Melo LG, Pratt RE, Ingwall JS, Dzau VJ. Evidence supporting paracrine hypothesis for akt-modified mesenchymal stem cell-mediated cardiac protection and functional improvement. *FASEB J.* 2006;20:661-669
76. Zsebo KM, Williams DA, Geissler EN, Broudy VC, Martin FH, Atkins HL, Hsu RY, Birkett NC, Okino KH, Murdock DC, et al. Stem cell factor is encoded at the sl locus of the mouse and is the ligand for the c-kit tyrosine kinase receptor. *Cell.* 1990;63:213-224
77. Kinnaird T, Stabile E, Burnett MS, Lee CW, Barr S, Fuchs S, Epstein SE. Marrow-derived stromal cells express genes encoding a broad spectrum of arteriogenic cytokines and promote in vitro and in vivo arteriogenesis through paracrine mechanisms. *Circ Res.* 2004;94:678-685
78. Kinnaird T, Stabile E, Burnett MS, Shou M, Lee CW, Barr S, Fuchs S, Epstein SE. Local delivery of marrow-derived stromal cells augments collateral perfusion through paracrine mechanisms. *Circulation.* 2004;109:1543-1549
79. Messina E, De Angelis L, Frati G, Morrone S, Chimenti S, Fiordaliso F, Salio M, Battaglia M, Latronico MV, Coletta M, Vivarelli E, Frati L, Cossu G, Giacomello A. Isolation and expansion of adult cardiac stem cells from human and murine heart. *Circ Res.* 2004;95:911-921
80. Chen X, Wilson RM, Kubo H, Berretta RM, Harris DM, Zhang X, Jaleel N, MacDonnell SM, Bearzi C, Tillmanns J, Trofimova I, Hosoda T, Mosna F, Cribbs L, Leri A, Kajstura J, Anversa P, Houser SR. Adolescent feline heart contains a population of small, proliferative ventricular myocytes with immature physiological properties. *Circ Res.* 2007;100:536-544
81. Anversa P, Loud AV, Levicky V, Guideri G. Left ventricular failure induced by myocardial infarction. II. Tissue morphometry. *Am J Physiol.* 1985;248:H883-889
82. Legato MJ. Cellular mechanisms of normal growth in the mammalian heart. II. A quantitative and qualitative comparison between the right and left ventricular myocytes in the dog from birth to five months of age. *Circ Res.* 1979;44:263-279
83. Mirotsou M, Zhang Z, Deb A, Zhang L, Gnechi M, Noiseux N, Mu H, Pachori A, Dzau V. Secreted frizzled related protein 2 (sfrp2) is the key

- akt-mesenchymal stem cell-released paracrine factor mediating myocardial survival and repair. *Proc Natl Acad Sci U S A.* 2007;104:1643-1648
84. Murry CE, Soonpaa MH, Reinecke H, Nakajima H, Nakajima HO, Rubart M, Pasumarthi KB, Virag JI, Bartelmez SH, Poppa V, Bradford G, Dowell JD, Williams DA, Field LJ. Haematopoietic stem cells do not transdifferentiate into cardiac myocytes in myocardial infarcts. *Nature.* 2004;428:664-668
  85. Nygren JM, Jovinge S, Breitbach M, Sawen P, Roll W, Hescheler J, Taneera J, Fleischmann BK, Jacobsen SE. Bone marrow-derived hematopoietic cells generate cardiomyocytes at a low frequency through cell fusion, but not transdifferentiation. *Nat Med.* 2004;10:494-501
  86. Bearzi C, Rota M, Hosoda T, Tillmanns J, Nascimbene A, De Angelis A, Yasuzawa-Amano S, Trofimova I, Siggins RW, Lecapitaine N, Cascapera S, Beltrami AP, D'Alessandro DA, Zias E, Quaini F, Urbanek K, Michler RE, Bolli R, Kajstura J, Leri A, Anversa P. Human cardiac stem cells. *Proc Natl Acad Sci U S A.* 2007;104:14068-14073
  87. Landa N, Miller L, Feinberg MS, Holbova R, Shachar M, Freeman I, Cohen S, Leor J. Effect of injectable alginate implant on cardiac remodeling and function after recent and old infarcts in rat. *Circulation.* 2008;117:1388-1396
  88. Segers VF, Lee RT. Biomaterials to enhance stem cell function in the heart. *Circ Res.* 2011;109:910-922
  89. Laflamme MA, Murry CE. Regenerating the heart. *Nat Biotechnol.* 2005;23:845-856
  90. Mohsin S, Khan M, Toko H, Bailey B, Cottage CT, Wallach K, Nag D, Lee A, Siddiqi S, Lan F, Fischer KM, Gude N, Quijada P, Avitabile D, Truffa S, Collins B, Dembitsky W, Wu JC, Sussman MA. Human cardiac progenitor cells engineered with pim-1 kinase enhance myocardial repair. *J Am Coll Cardiol.* 2012;60:1278-1287
  91. Quijada P, Toko H, Fischer KM, Bailey B, Reilly P, Hunt KD, Gude NA, Avitabile D, Sussman MA. Preservation of myocardial structure is enhanced by pim-1 engineering of bone marrow cells. *Circ Res.* 2012;111:77-86
  92. Kleinman HK, Martin GR. Matrigel: Basement membrane matrix with biological activity. *Semin Cancer Biol.* 2005;15:378-386

93. Kofidis T, Lebl DR, Martinez EC, Hoyt G, Tanaka M, Robbins RC. Novel injectable bioartificial tissue facilitates targeted, less invasive, large-scale tissue restoration on the beating heart after myocardial injury. *Circulation*. 2005;112:I173-177
94. Ott HC, Matthiesen TS, Goh SK, Black LD, Kren SM, Netoff TI, Taylor DA. Perfusion-decellularized matrix: Using nature's platform to engineer a bioartificial heart. *Nat Med*. 2008;14:213-221
95. Pham C, Greenwood J, Cleland H, Woodruff P, Maddern G. Bioengineered skin substitutes for the management of burns: A systematic review. *Burns*. 2007;33:946-957
96. Atala A, Bauer SB, Soker S, Yoo JJ, Retik AB. Tissue-engineered autologous bladders for patients needing cystoplasty. *Lancet*. 2006;367:1241-1246
97. Yu J, Vodyanik MA, Smuga-Otto K, Antosiewicz-Bourget J, Frane JL, Tian S, Nie J, Jonsdottir GA, Ruotti V, Stewart R, Slukvin, II, Thomson JA. Induced pluripotent stem cell lines derived from human somatic cells. *Science*. 2007;318:1917-1920
98. Takahashi K, Tanabe K, Ohnuki M, Narita M, Ichisaka T, Tomoda K, Yamanaka S. Induction of pluripotent stem cells from adult human fibroblasts by defined factors. *Cell*. 2007;131:861-872
99. Jugdutt BI. Ventricular remodeling after infarction and the extracellular collagen matrix: When is enough enough? *Circulation*. 2003;108:1395-1403